Supporting Information

Polymer Networks Based on Photo-Caged Diene Dimerization

Tim Krappitz, Florian Feist, Iris Lamparth, Norbert Moszner, Hendrik John, James Blinco, Tim R. Dargaville, Christopher Barner-Kowollik*

S1 Experimental Section

NMR-spectroscopy

^{1}H, ^{13}C-NMR as well as COSY, HSQC and HMBC-spectra were recorded on a Bruker System 600 Ascend LH, equipped with an BBO-Probe (5 mm) with z-gradient (^{1}H: 600.13 MHz, ^{13}C: 150.90 MHz). The δ-scale was normalized relative to the solvent signal of $CHCl_3$ or DMSO for ^{1}H spectra and for ^{13}C spectra on the middle signal of $CHCl_3$ triplett, the DMSO quintett. The annotation of the resonances is based on COSY, HSQC and HMBC-experiments.

Size-Exclusion Chromatography

The SEC measurements were conducted on a PSS SECurity system consisting of a PSS SECurity Degasser, PSS SECurity TCC6000 Column Oven (60 °C), PSS GRAM Column Set (8x150 mm 10 µm Precolumn, 8x300 mm 10 µm Analytical Columns, 1000 Å, 1000 Å and 30 Å) and an Agilent 1260 Infinity Isocratic Pump, Agilent 1260 Infinity Standard Autosampler, Agilent 1260 Infinity Diode Array and Multiple Wavelength Detector (A: 25415 nm, B: 360 nm), Agilent 1260 Infinity Refractive Index Detector (35 °C). HPLC grade DMAc, 0.01 M LiBr, is used as eluent at a flow rate of 1 mL·min^{-1}. Narrow disperse linear poly(methyl methacrylate) (M_n: 202 g·mol^{-1} to 2.2×106 g·mol^{-1}) standards (PSS ReadyCal) were used as calibrants. All samples were passed over 0.22 µm PTFE membrane filters. Molecular weight and dispersity analysis was performed in PSS WinGPC UniChrom software (version 8.2).

Differential Scanning Calorimetry

Differential Scanning Calorimetry was done with a Q100 DSC V9.6 Build 290 from TA Instruments, measurements were cycled twice from -40 °C to 120 °C, unless stated otherwise, at 10 °C min^{-1}. A nitrogen sample purge flow of 50 mL min^{-1} was utilized. The T_g was determined at the point of inflection via TA Instruments Universal Analysis 2000 software (version 4.2E).

Thermogravimetric Analysis

Thermogravimetric Analysis was performed on a Q500 TGA V6.5 Build 196 from TA Instruments. The heating under air from 30 °C to 800 °C at 10 °C min^{-1} was recorded.

Rheology

Rheology was measured on an Anton Parr MCR 302 Rheometer equipped with a PP25 measuring system. The shear gap was set to 0.05 mm and the temperature to 140 °C. After several minutes for temperature equilibration, the samples were investigated at a constant shear strain of 1% and an angular frequency of 10 rad s^{-1}. Irradiation was done with an OmniCure S1000 light source equipped

with a fibre light guide with a 365 nm EXFO-UV bandpass filter through the bottom plate, constituting of quartz glass (80 $mW \cdot cm^{-2}$).

Radiometer

Stated irradiance values in $mW \cdot cm^{-2}$ were determined from an ILT1400 Radiometer Photometer equipped with SEL005 detector and a WBS320 filter for the UV range. The stated irradiance value for the visible region was measured with a SPIC-200BW (380-780 nm) with an OD1.5 neutral density filter in place to avoid saturation.

Nanoindentation

The mechanical properties were tested *via* load controlled indentation using a Hysitron TL950 Nanoindentor equipped with a Berkovich Tip. The measurements were done at ambient conditions. Each indentation was done with 2000 µN peak force and a 1 s load, 2 s hold, 1 s unload program. The *Oliver and Pharr* method was utilized for analysis and the determined values for the reduced E-modulus and hardness were averaged from at least 5 measurements each.

Flow Reactions

Photoreactions under continuous flow conditions were performed using a Vapourtec E-series platform (peristaltic pumps) in combination the UV-150 module and the VSD006 cooling module. The module consists of a temperature controlled irradiation chamber, a transparent fluorinated ethylene polymer (FEP) reactor coil (1.3 mm inner diameter, 0.15 mm wall thickness, 10 mL PN: 50-1287) and a LED assembly (360 to 390 nm, peak 365 nm, total power output of 16 W, PN: 50-4036). The temperature is controlled employing pre-cooled nitrogen (heat exchange in the cooling module).

Flash Chromatography

Flash chromatography was performed on a *Interchim* XS420+ flash chromatography system consisting of a SP-in-line filter 20-µm, an UV-VIS detector (200-800 nm) and a *SofTA* Model 400 ELSD (55 °C dift tube temperature, 25 °C spray chamber temperature, filter 5, EDR gain mode) connected via a flow splitter (*Interchim* Split ELSD F04590). The separations were performed using a *Interchim* dry load column (dryload on celite 565) and a *Interchim* Puriflash Silica HP 30 µm column or a *Interchim* Uptisphere Strategy SI 10 µm column respectively.

LC-MS measurements

LC-MS measurements were performed on a UltiMate 3000 UHPLC system (Dionex, Sunnyvale, CA, USA) consisting of a pump (LPG 3400SZ, autosampler WPS 3000TSL) and a temperature controlled column department (TCC 3000). Separation was performed on a C18 HPLC-column (Phenomenex Luna 5µm, 100 Å, 250 × 2.0 mm) operating at 40 °C. A gradient of ACN:H_2O 60:40 – 90:10 *v/v* at a flow rate of 0.20 $mL \cdot min^{-1}$ during 15 min was used as the eluting solvent. The flow was split in a 9:1 ratio, where 90 % (0.18 $mL \cdot min^{-1}$) of the eluent were directed through the UV-detector (VWD 3400, Dionex, detector wavelengths 215, 254, 280, 360 nm) and 10 % (0.02 $mL \cdot min^{-1}$) were infused into the electrospray source. Spectra were recorded on a LTQ Orbitrap Elite mass spectrometer (Thermo Fisher Scientific, San Jose, CA, USA) equipped with an HESI II probe. The instrument was calibrated in the *m/z* range 74-1822 using premixed calibration solutions (Thermo Scientific). A constant spray voltage of 3.5 kV, a dimensionless sheath gas and a dimensionless auxiliary gas flow rate of 5 and 2 were applied,

respectively. The capillary temperature and was set to 300 °C, the S-lens RF level was set to 68, and the aux gas heater temperature was set to 125 °C.

Example procedure for the polymerization of prepolymers

To a solution of 0.47 g methyl methacrylate (4.7 mmol, 7.50 eq), 2.9 g butyl methacrylate (20.4 mmol, 33.00 eq.) and 2.4 g of PEMA (6.2 mmol, 10.00 eq) in 50 mL toluene were added 103 mg of 2,2'-azobisisobutyronitrile (AIBN, 0.6 mmol, 1.00 eq) and 150 µL lauryl mercaptan (0.62 mmol, 2.00 eq). The reaction mixture was purged for 20 min with nitrogen and the reaction started at 65 °C. The reaction mixture was quenched with 1 mL of a 10 wt% solution of hydroquinone in tetrahydrofuran and rapid cooling as well as exposure to air. The polymer was repeatedly precipitated in an excess of a mixture of cold methanol in water (v/v 10/1) and dried in vacuum.

Photopolymerization & Crosslinking

The respective monomer mixture (200.00 eq) and phenylbis(2,4,6-trimethylbenzoyl)-phosphine (^{Mes}BAPO-Ph, 1.00 eq) was fully dissolved at 50 °C or below, depending on the solubility of the solid compounds (PEMA and ^{Mes}BAPO-Ph) in the respective co-monomer composition. Subsequently, 0.8 mL of the reaction solution were syringed into an aluminum dish with a diameter of 2.5 cm and irradiated from the top in a Luzchem LZC-4V photoreactor using 6 x LZC-LBL lamps, emitting at ~445-465 nm. The intensity was measured to be 7 mW/cm^2. For UV-irradiation, LZC-UVA lamps with an emission centered at ~350 nm were utilized. 6 x 8W lamps were installed for top irradiation. The intensity was measured to be 5 mW/cm^2.

S2 Chemicals

Chemicals were used as received without further purification if not stated otherwise: sodium sulfate (99.5 %, Chem-Supply), *N*,*N*-dimethylformamide (DMF, anhydrous 99.8 %, Sigma-Aldrich), 1-ethyl-3-(3-dimethylaminopropyl)carbodiimide hydrochloride (EDC HCl, 98 %, Sigma-Aldrich), 4-(dimethylamino)pyridine (DMAP, 98%, Merck), tetraethylene glycol (TEG, 99%, Sigma-Aldrich), ethyl hydrogen fumarate (97%, Fisher), methyl methacrylate (MMA, 99%, Sigma-Aldrich), butyl methacrylate (BMA, 99%, Sigma-Aldrich), isobornyl methacrylate (IBOMA, technical grade, Sigma-Aldrich), tetrahydrofurfuryl methacrylate (THFMA, 97%, Sigma-Aldrich), methyl acrylate (MA, 99%, Fisher), acetonitrile (HPLC-grade, Fisher), dimethyl sulfoxide (DMSO, anhydrous 99,9 %, Sigma-Aldrich), methanol (analytical reagent, Ajax Finechem), THF (analytical reagent, Fisher), chloroform (analytical reagent, Fisher), cyclohexane (CH, analytical reagent, Ajax Finechem), ethyl acetate (EE, analytical reagent, Fisher), dichloromethane (DCM, analytical reagent, Fisher), acetonitrile-d^3 (99.8 %D, Cambridge Isotope Laboratories), chloroform-d (99.8 %D, Cambridge Isotope Laboratories), dimethylsulfoxide-d^6 (99.9 %D, Cambridge Isotope Laboratories).

S3 Synthesis

S3.1 Synthesis of 2-methoxy-6-methylbenzaldehyde (**PE-OMe**)

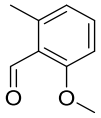

PE-OMe

2-methoxy-6-methylbenzaldehyde was synthesized according to a literature known procedure.[1,2] To obtain it in a suitable purity (evidenced by LC-MS and NMR spectroscopy: Fig. S14 and Fig. S26) it was additionally purified using a *Interchim* Uptisphere Strategy SI 10 µm column (gradient: pentane/ethyl acetate 5:95-15:85 *v/v*).

^{1}H NMR (600 MHz, $CDCl_3$) δ 10.65 (s, 1H), 7.38 (t, *J* = 8.0 Hz, 1H), 6.84 (d, *J* = 8.4 Hz, 1H), 6.81 (d, *J* = 7.3 Hz, 1H), 3.90 (s, 3H), 2.57 (s, 3H).

S3.2 Synthesis of diethyl *O,O'*-(((oxybis(ethane-2,1-diyl))bis(oxy))bis(ethane-2,1-diyl)) difumarate

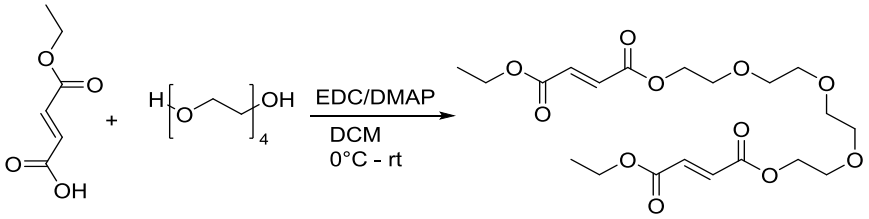

4.48 g of mono-ethyl fumarate (31.1 mmol, 2.30 eq) and 0.50 g 4-dimethylaminopyridine (4.06 mmol, 0.30 eq) were dissolved in 70 mL dry dichloromethane and 2.63 g tetraethylene glycol (13.5 mmol, 1.00 eq) were added. The solution was cooled to 0 °C and 7.79 g N-(3-dimethylaminopropyl)-N'-ethylcarbodiimide hydrochloride (40.56 mmol, 3.00 eq) were slowly added. The reaction mixture was stirred at room temperature for 15 hours. The organic phase was washed three times with water and dried over magnesium sulfate. The crude product was purified by column chromatography on silica gel (cyclohexane:ethyl acetate 4:1 *v/v*). The product was obtained as colourless liquid, 3.98 g (66% yield).

^{1}H NMR (600 MHz, $CDCl_3$) δ 6.81 (d, 4H), 4.30 – 4.27 (m, 4H), 4.19 (q, *J* = 7.1 Hz, 4H), 3.70-3.67 (m, 4H), 3.60 (s, 8H), 1.25 (t, 6H).

^{13}C NMR (150 MHz, $CDCl_3$) δ 164.94, 164.89, 134.06, 133.25, 70.68, 70.66, 68.93, 64.41, 61.38, 14.12.

S3.3 Synthesis of 2-(methacryloyloxy)ethyl 4-((2-formyl-3-methylphenoxy)-methyl)-benzoate (**PEMA**)

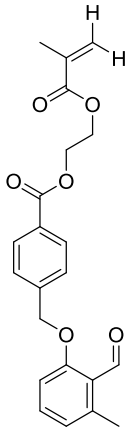

PEMA

PEMA was synthesized according to a literature known procedure.[3]

^{1}H NMR (600 MHz, DMSO-d^{6}) δ 10.63 (d, *J* = 0.6 Hz, 1H), 7.98 (d, *J* = 8.3 Hz, 2H), 7.66 – 7.62 (m, 2H), 7.47 (dd, *J* = 8.4, 7.6 Hz, 1H), 7.12 (d, *J* = 8.5 Hz, 1H), 6.89 (dd, *J* = 7.6, 0.8 Hz, 1H), 6.03 (dd, *J* = 1.7, 1.0 Hz, 1H), 5.68 (p, *J* = 1.6 Hz, 1H), 5.35 (s, 2H), 4.57 – 4.51 (m, 2H), 4.48 – 4.40 (m, 2H), 2.48 (s, 3H), 1.86 (dd, *J* = 1.6, 1.0 Hz, 3H).

^{13}C NMR (151 MHz, DMSO-d^{6}) δ 191.57, 166.41, 165.33, 161.42, 142.27, 140.70, 135.61, 134.79, 129.44, 128.94, 127.45, 126.11, 124.22, 123.09, 111.36, 69.29, 62.66, 62.37, 20.83, 17.92.

S4 Photoflow Experiments

S4.1 Temperature Study of the **PE-OMe** Dimerization under Flow Conditions.

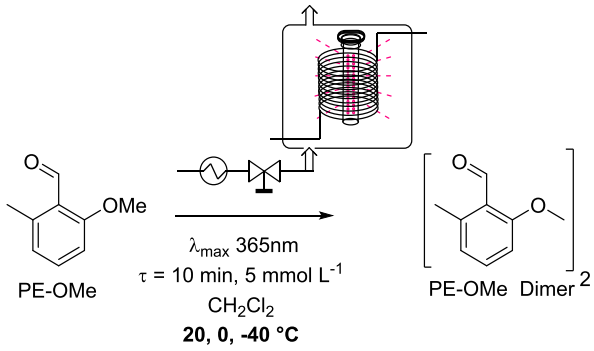

The photoflow reactions were performed using a flow reactor described in the experimental section. PE-OMe (15.01 mg, 0.1 mmol) was dissolved in 20 mL (c = 5 mmol L^{-1}) dichloromethane. The reaction mixture was deoxygenated by passing through nitrogen for 10 min. Afterwards the solution was irradiated in a flow reactor (5 mL PFA-coil) with a retention time (τ) of 10 min (flow rate: 0.5 mL min^{-1}) at different reactor temperatures (20 °C, 0 °C, -40 °C). The reaction mixture was collected under inert atmosphere and the volatiles were removed under reduced pressure at room temperature. The product was analysed by ^{1}H NMR spectroscopy (Fig. S1 and S26 respectively).

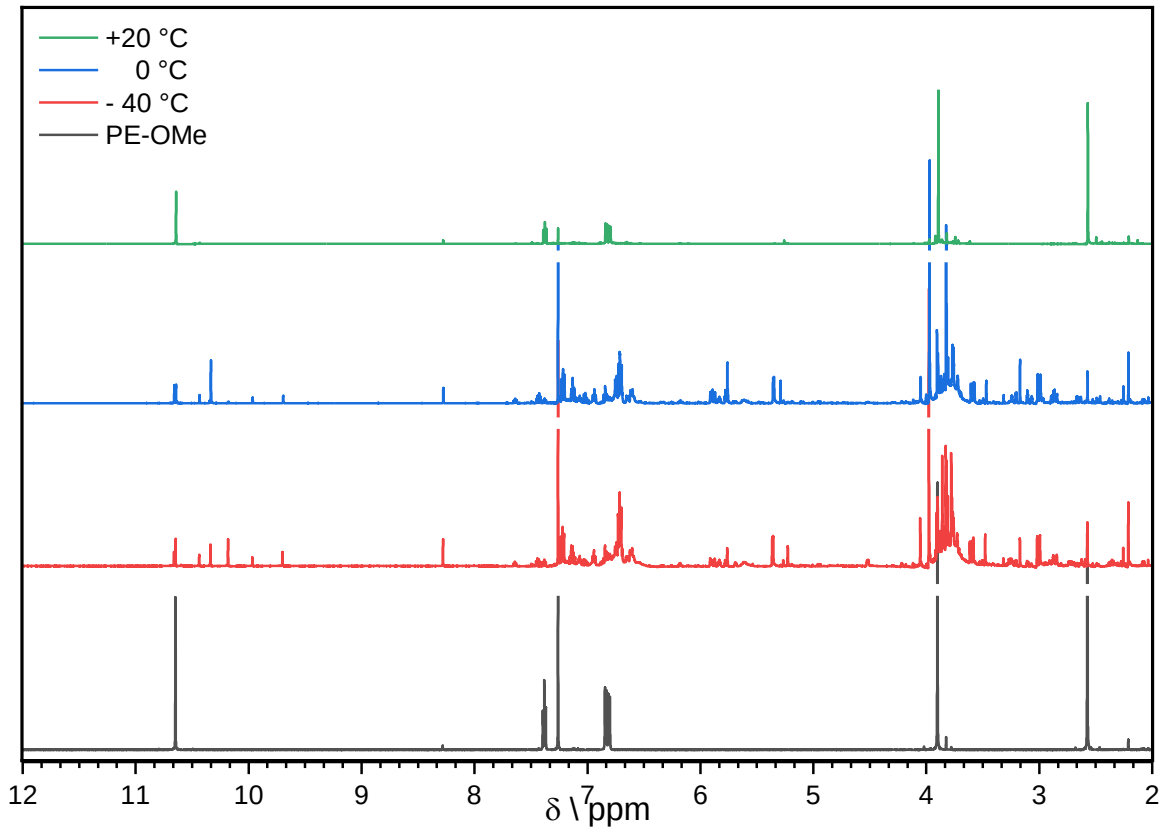

Fig. S1: ^{1}H NMR spectra of the crude materials obtained in the photoreactions with PE-OMe at different temperatures in comparison to the starting material. At room temperature almost no conversion occurred (green line). At 0 °C and -40 °C (blue and red line) the starting material is almost completely converted to a variety of products. See Fig. S2 for detailed carbonyl region.

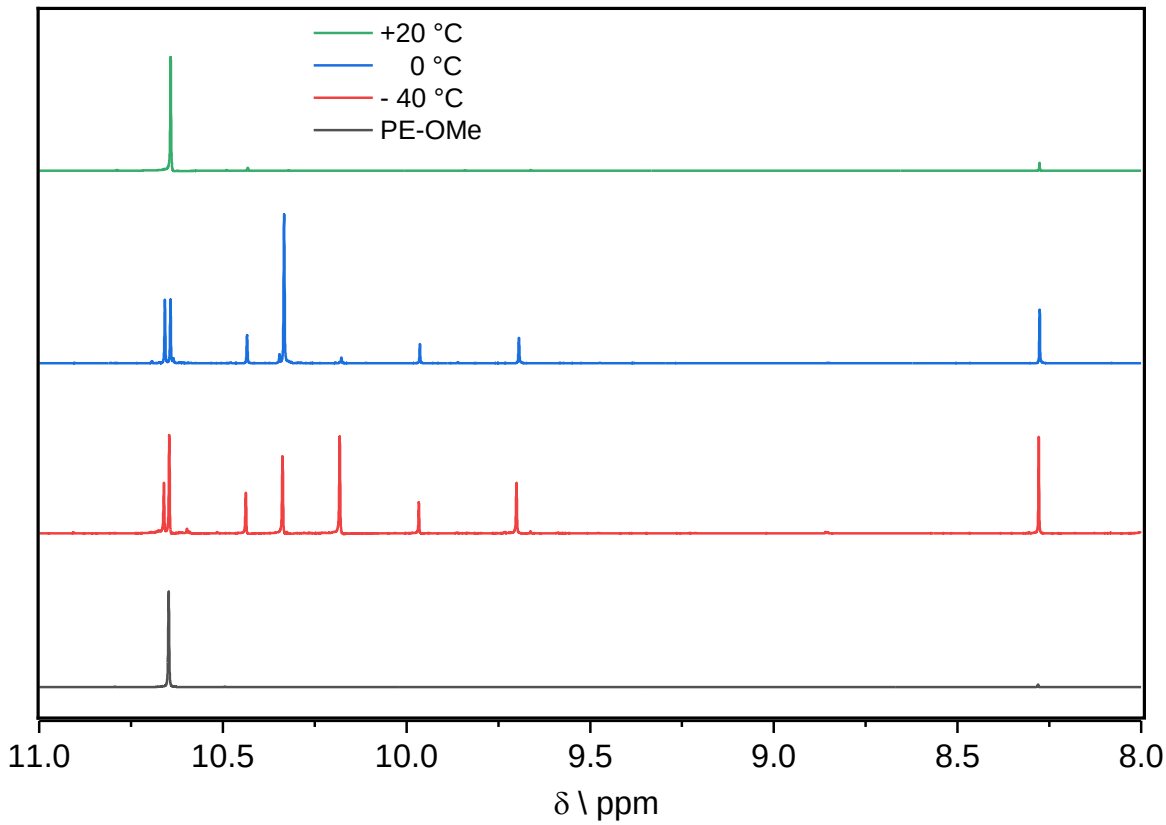

Fig. S2: Detailed ^{1}H-NMR spectrum of the carbonyl region (8.0-11.0 ppm) of the crude materials obtained in the photoreactions with **PE-OMe** at different temperatures.

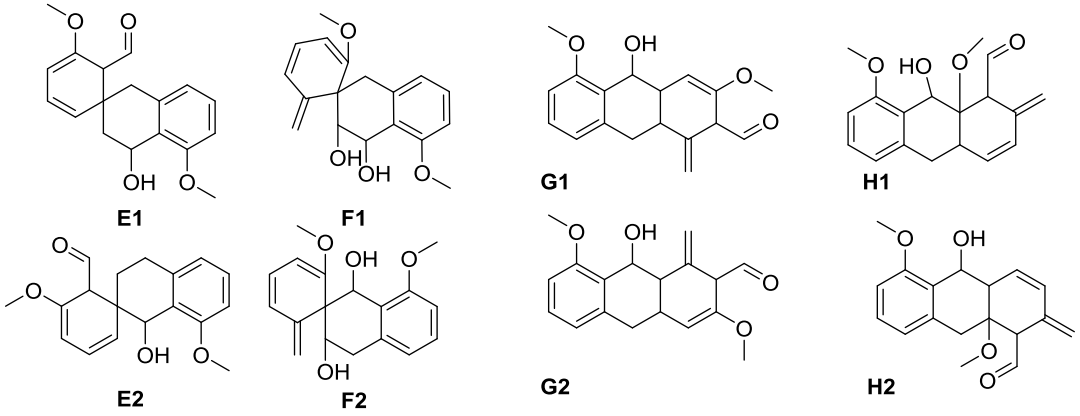

Scheme S1: [4+2]-cycloadducts (**E1 – H2**) causing the characteristic NMR resonances in **Fig. S2**. The products were not isolated and characterized in the course of the study. We assume that the products are not stable and might decompose or react during the workup procedure.

S4.2 Solvent Study of the **PE-OMe** Dimerization under Flow Conditions

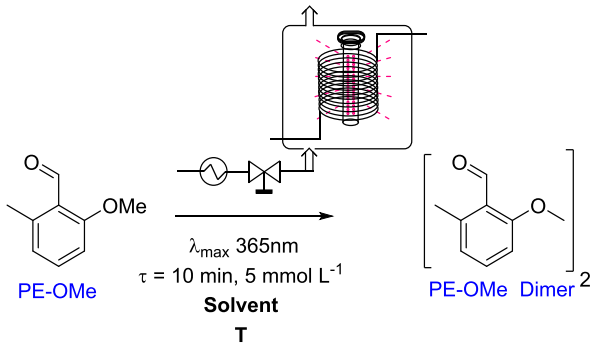

The photoflow reactions were performed using a flow reactor described in the experimental section. **PE-OMe** (15.01 mg, 0.1 mmol) was dissolved in 20 mL (c = 5 mmol L^{-1}) of the solvent (DMSO, DCM, ethyl acetate, toluene). The reaction mixture was deoxygenated by passing through nitrogen for 10 min. Afterwards the solution was irradiated in a flow reactor (5 mL PFA-coil) with a retention time (τ) of 10 min (flow rate: 0.5 mL min^{-1}) at different reactor temperatures (DCM, ethyl acetate, toluene: -40 °C, DMSO 20 °C). The reaction mixture was collected under inert atmosphere and the volatiles were removed under reduced pressure at room temperature. The product was analysed by ^{1}H NMR spectroscopy (Fig. S3).

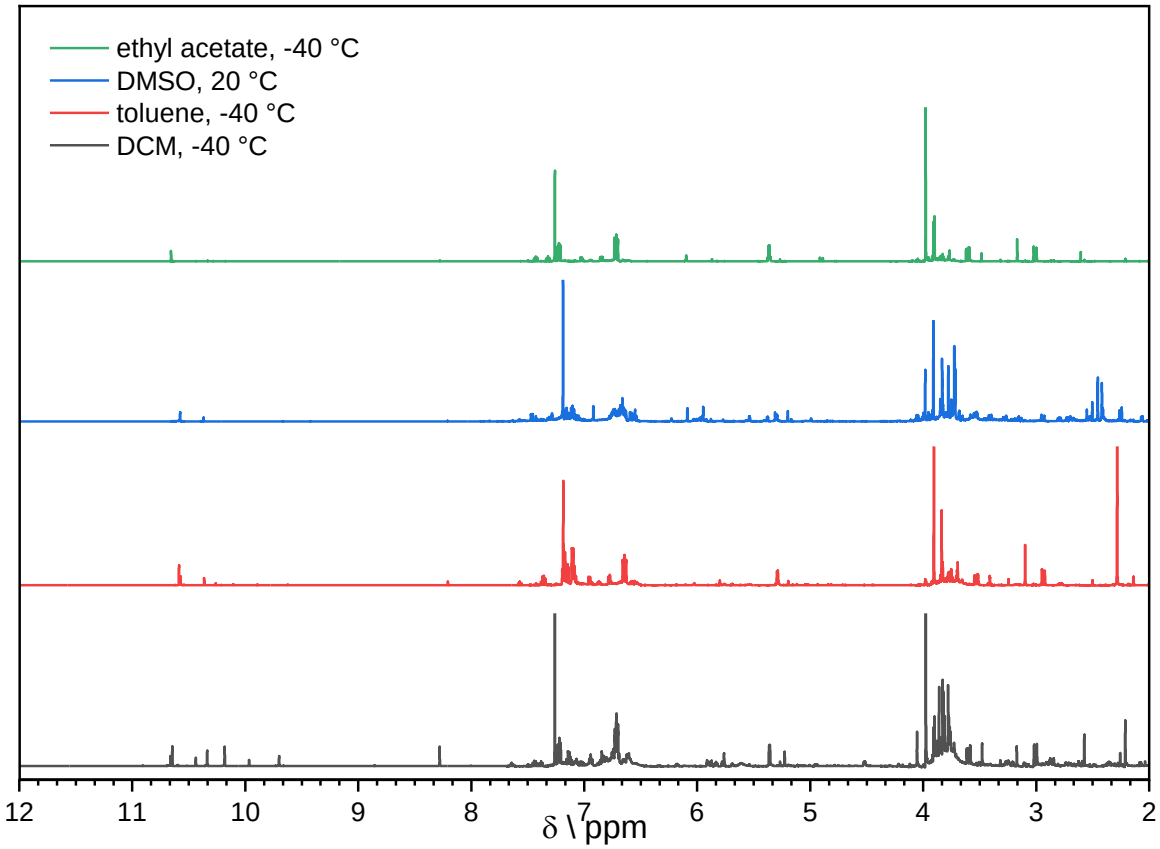

Fig. S3: ^{1}H NMR spectra (recorded in $CDCl_3$) of the crude materials obtained in different solvents (green: ethyl acetate, -40 °C; blue: DMSO, 20 °C; red: toluene, -40 °C; black, DCM, -40 °C). Conversion of the starting material occurred in all cases. Largely different product ratios were observed.

S4.3. Preparative Photoflow Reaction and Isolation of the Major Dimerization Products of PE-OMe

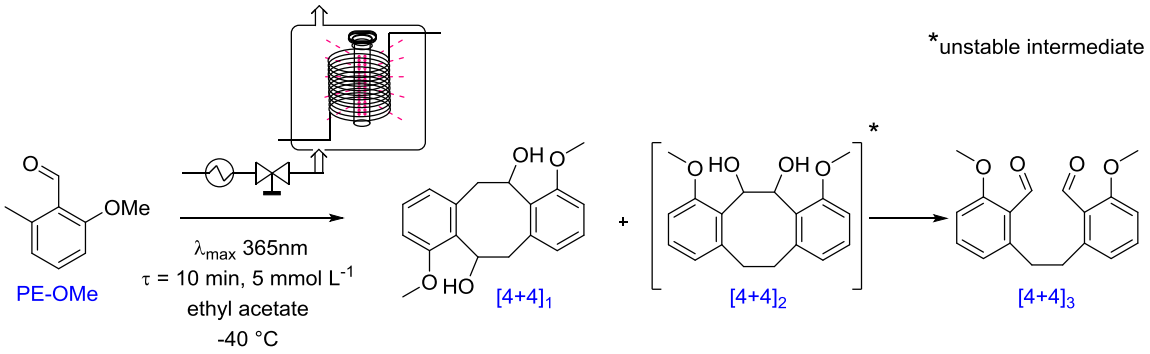

PE-OMe (52.52 mg, 0.350 mmol) were dissolved in 70 mL (*c* = 5 mmol L^{-1}) ethyl acetate. The reaction mixture is deoxygenated by passing through nitrogen for 10 min. Afterwards the solution was irradiated in a flow reactor equipped with a 10 mL PFA-coil with a retention time (τ) of 10 min (flow rate: 1 mL min^{-1}) at -40 °C. The reaction mixture was collected under inert atmosphere and the volatiles were removed under reduced pressure at room temperature. The crude product was analysed by LC-MS (Fig. S30) and NMR spectroscopy (Fig. S3). Subsequently the dimerization products were isolated employing flash column chromatography (stationary phase: *Interchim* Uptisphere Strategy SI 10 µm column; gradient: pentane/ethyl acetate 95:5-15:85 *v/v*).

Isolated products:

[4+4]$_1$ (4,10-dimethoxy-5,6,11,12-tetrahydrodibenzo[*a,e*][8]annulene-5,11-diol)

The product was obtained as colourless solid.

^{1}H NMR (600 MHz, $CDCl_3$) δ 7.25 – 7.19 (m, 2H), 6.73 (d, *J* = 7.1 Hz, 2H), 6.71 (d, *J* = 8.4 Hz, 2H), 5.35 (dd, *J* = 4.6, 1.8 Hz, 2H), 3.97 (d, *J* = 0.8 Hz, 6H), 3.60 (ddd, *J* = 14.4, 4.5, 0.8 Hz, 2H), 3.00 (dd, *J* = 14.4, 1.0 Hz, 2H), 2.24 (s, 2H).

^{13}C NMR (151 MHz, $CDCl_3$) δ 154.47, 144.23, 131.48, 131.07, 115.80, 113.94, 70.89, 57.04, 42.69.

[4+4]$_3$ (6,6'-(ethane-1,2-diyl)bis(2-methoxybenzaldehyde)

The product was obtained as colourless solid.

^{1}H NMR (600 MHz, $CDCl_3$) δ 10.66 (d, *J* = 0.6 Hz, 2H), 7.43 (dd, *J* = 8.3, 7.6 Hz, 2H), 7.03 (d, *J* = 7.6 Hz, 2H), 6.85 (dd, *J* = 8.4, 0.9 Hz, 2H), 3.91 (s, 6H), 3.17 (s, 4H).

^{13}C NMR (151 MHz, $CDCl_3$) δ 192.45, 163.29, 145.90, 134.84, 124.01, 123.16, 109.39, 55.96, 35.55.

S5 NMR spectra

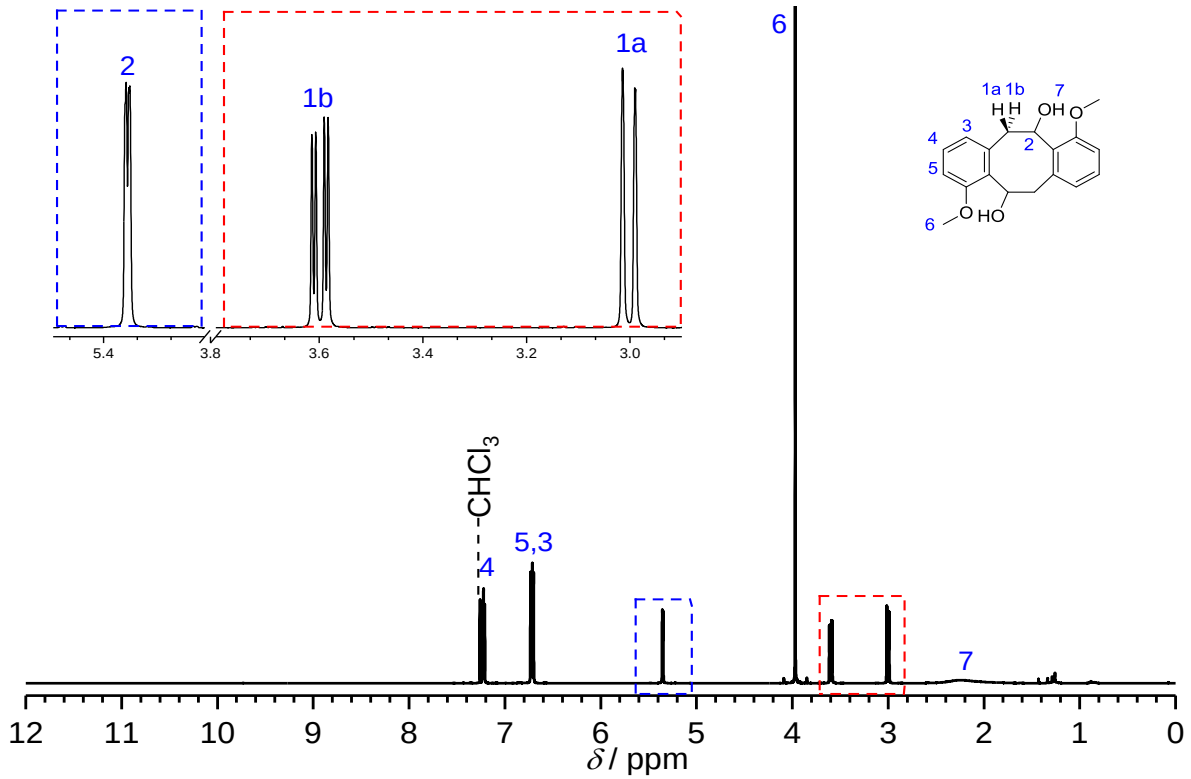

Fig. S4: ^{1}H NMR spectrum of 4,10-dimethoxy-5,6,11,12 tetrahydrodibenzo[*a,e*][8]-annulene-5,11-diol (**[4+4]$_1$**) in $CDCl_3$.

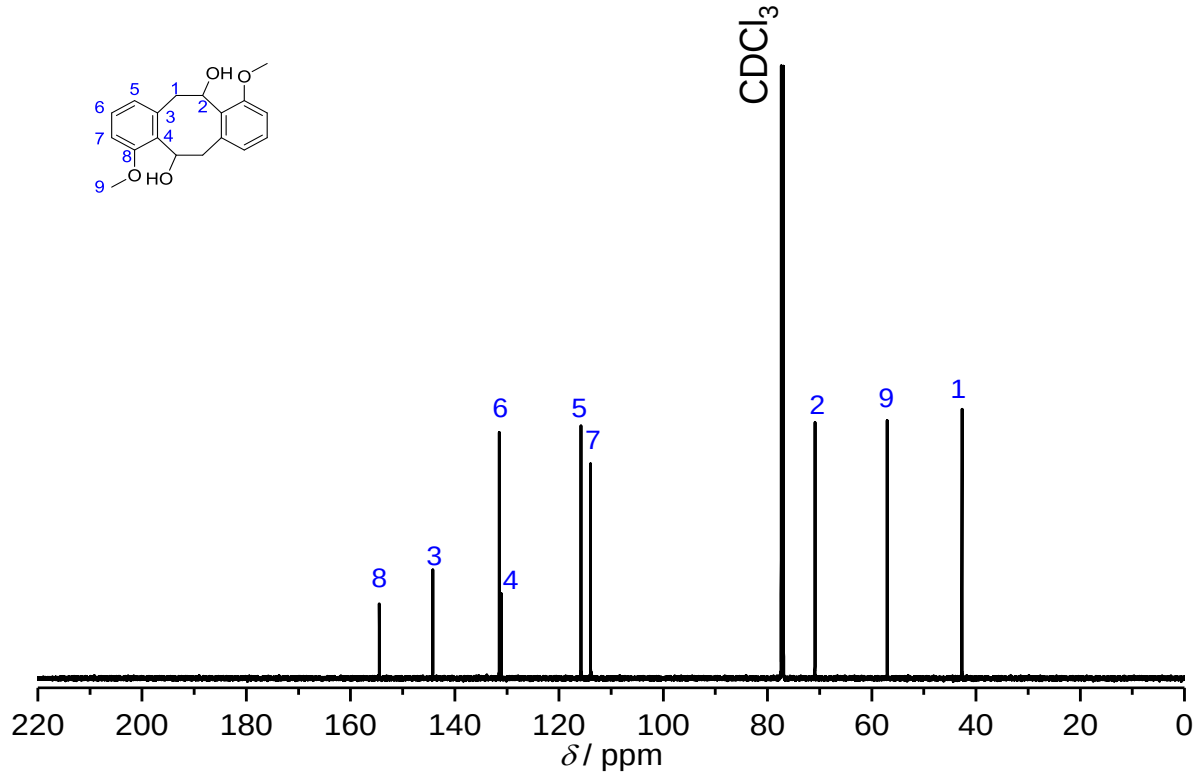

Fig. S5: ^{13}C NMR spectrum of 4,10-dimethoxy-5,6,11,12-tetrahydrodibenzo[*a,e*][8]-annulene-5,11-diol (**[4+4]$_1$**) in $CDCl_3$.

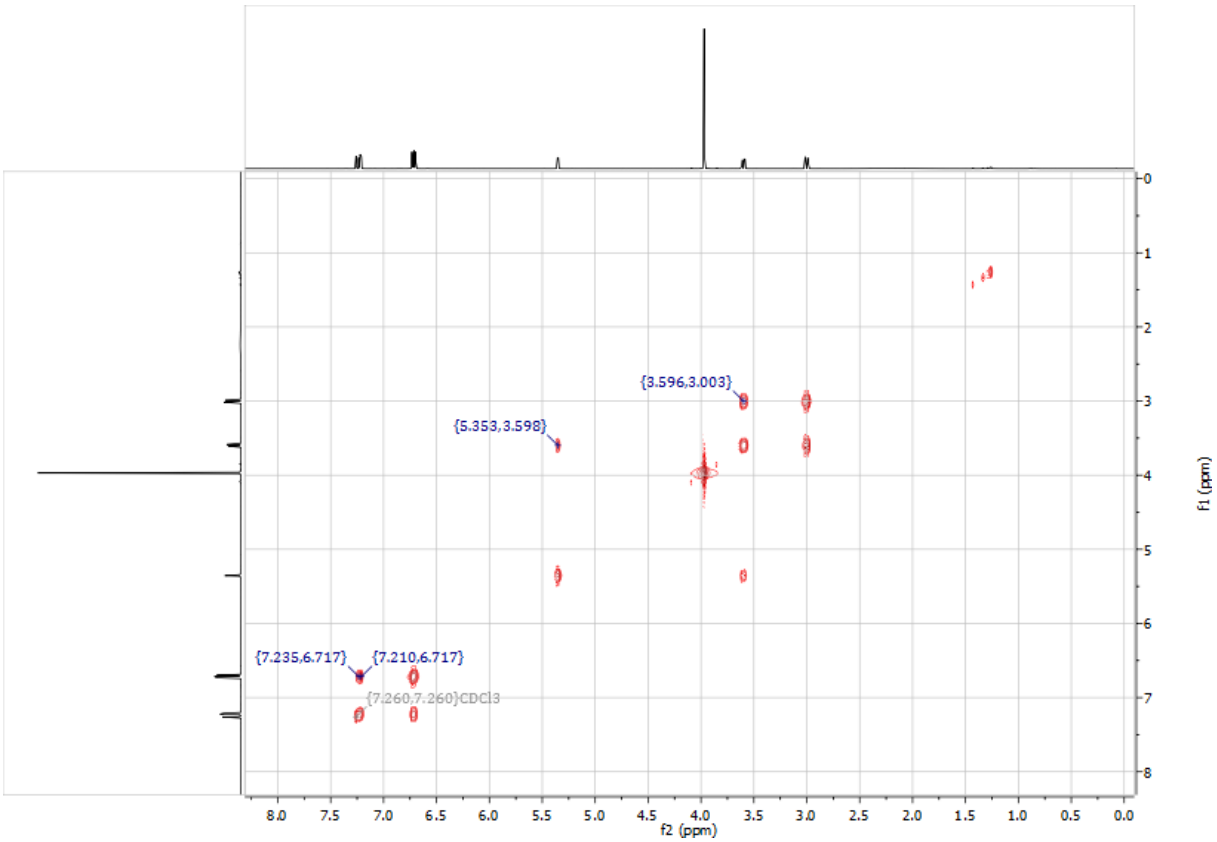

Fig. S6: COSY spectrum of 4,10-dimethoxy-5,6,11,12-tetrahydrodibenzo[*a,e*][8]annulene-5,11-diol (**[4+4]**$_1$) in $CDCl_3$.

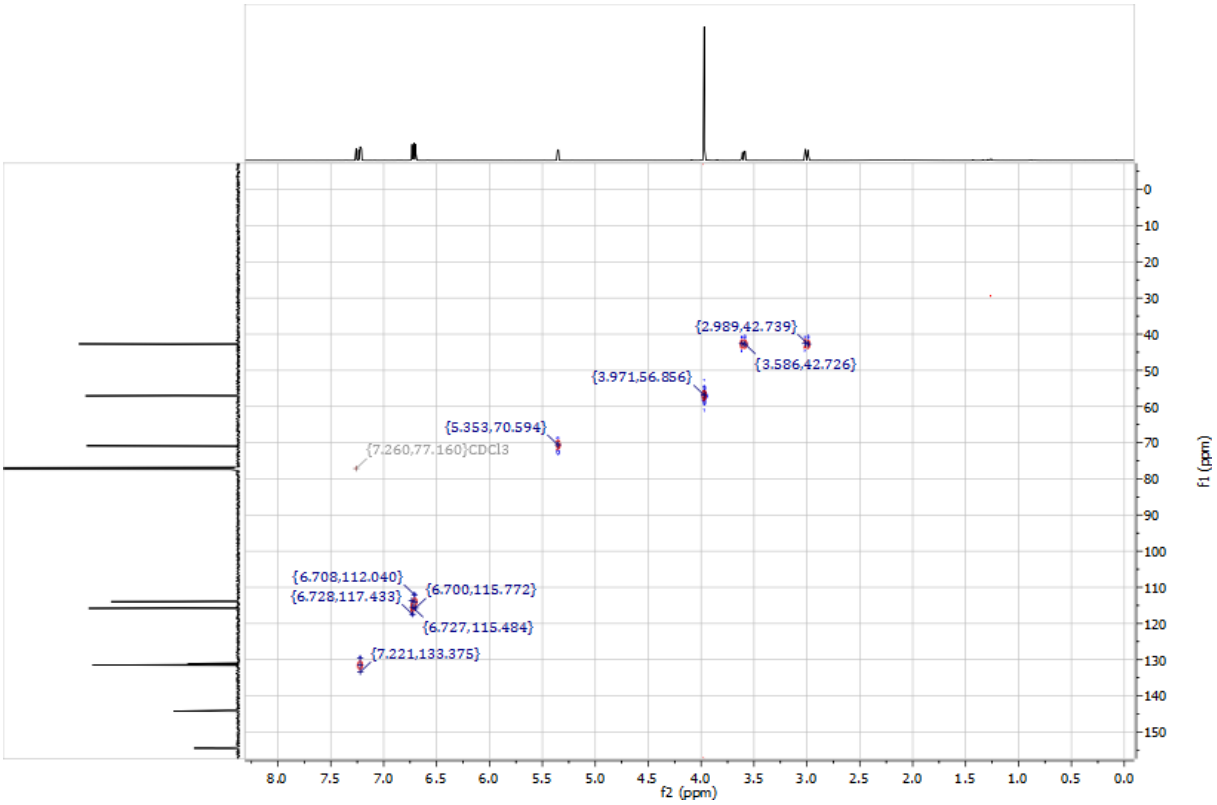

Fig. S7: HSQC spectrum of 4,10-dimethoxy-5,6,11,12-tetrahydrodibenzo[*a,e*][8]annulene-5,11-diol (**[4+4]**$_1$) in $CDCl_3$.

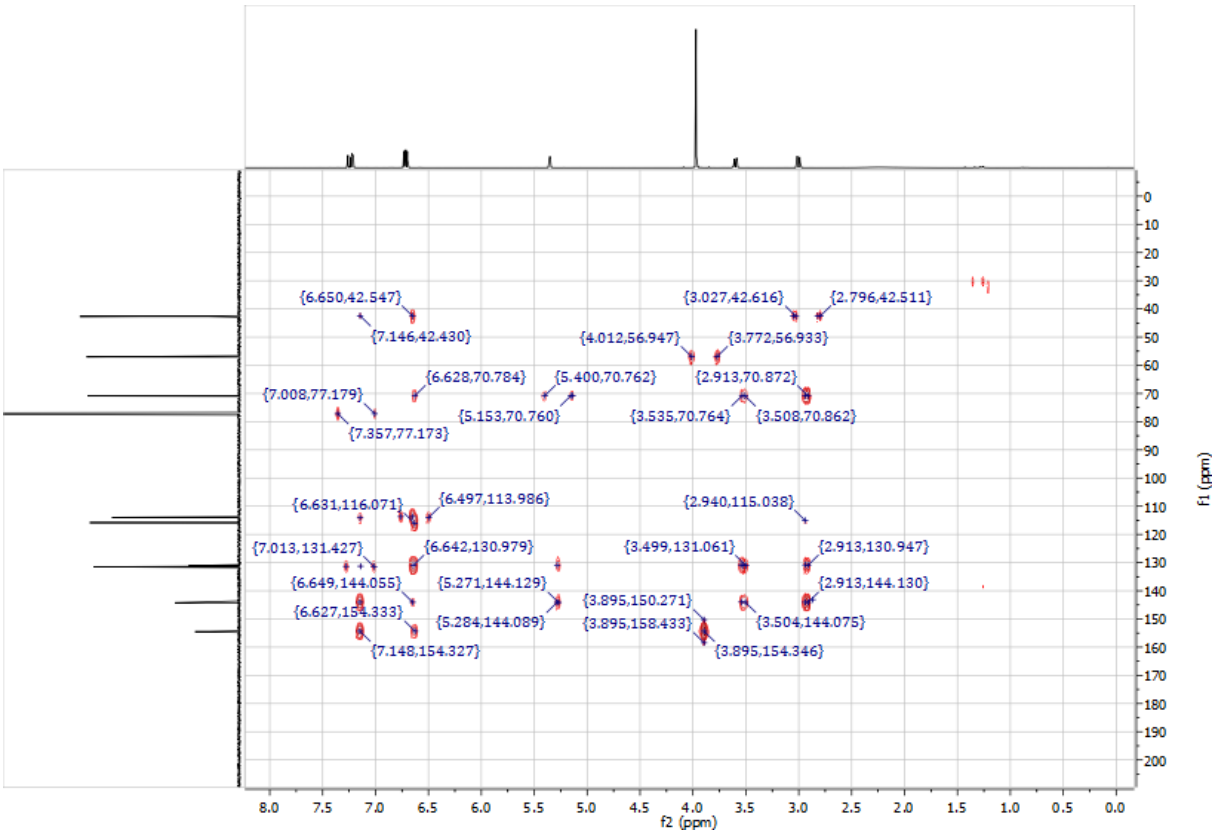

Fig. S8: HMBC spectrum of 4,10-dimethoxy-5,6,11,12-tetrahydrodibenzo[*a,e*][8]-annulene-5,11-diol (**[4+4]$_1$**) in $CDCl_3$.

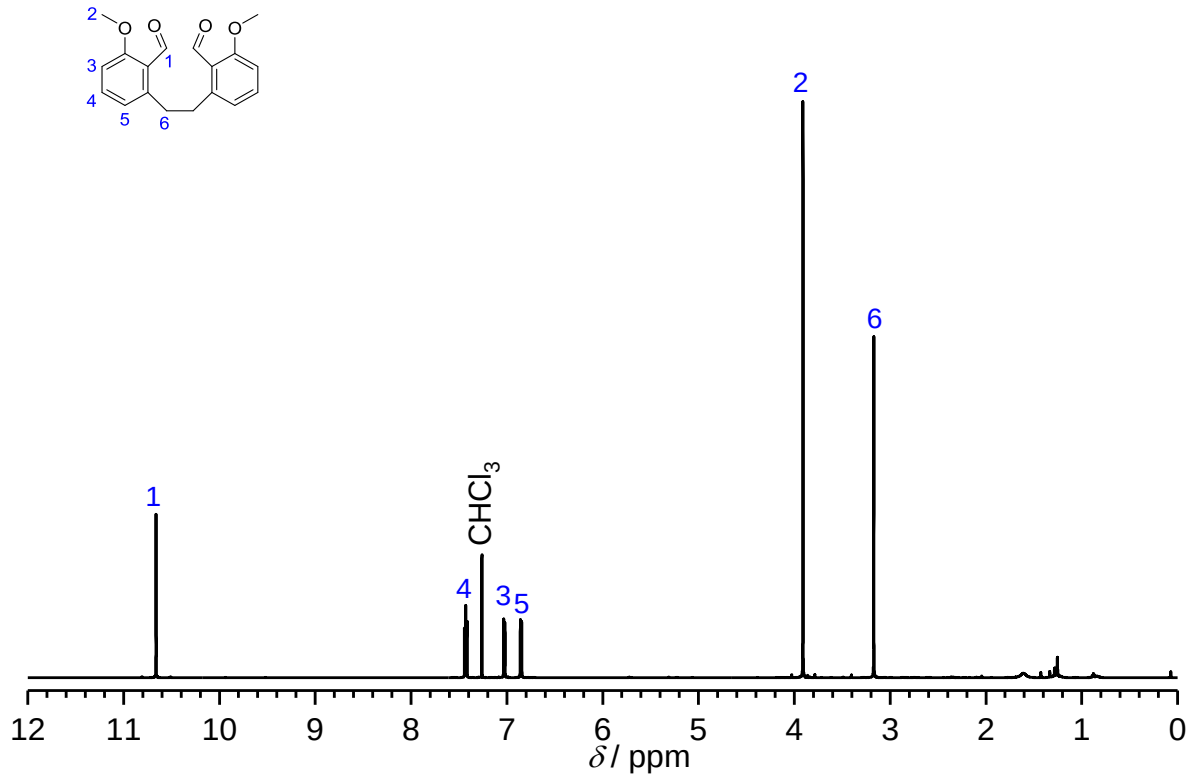

Fig. S9: ^{1}H NMR spectrum of 6,6'-(ethane-1,2-diyl)bis(2-methoxybenzaldehyde) (**[4+4]$_3$**) in $CDCl_3$.

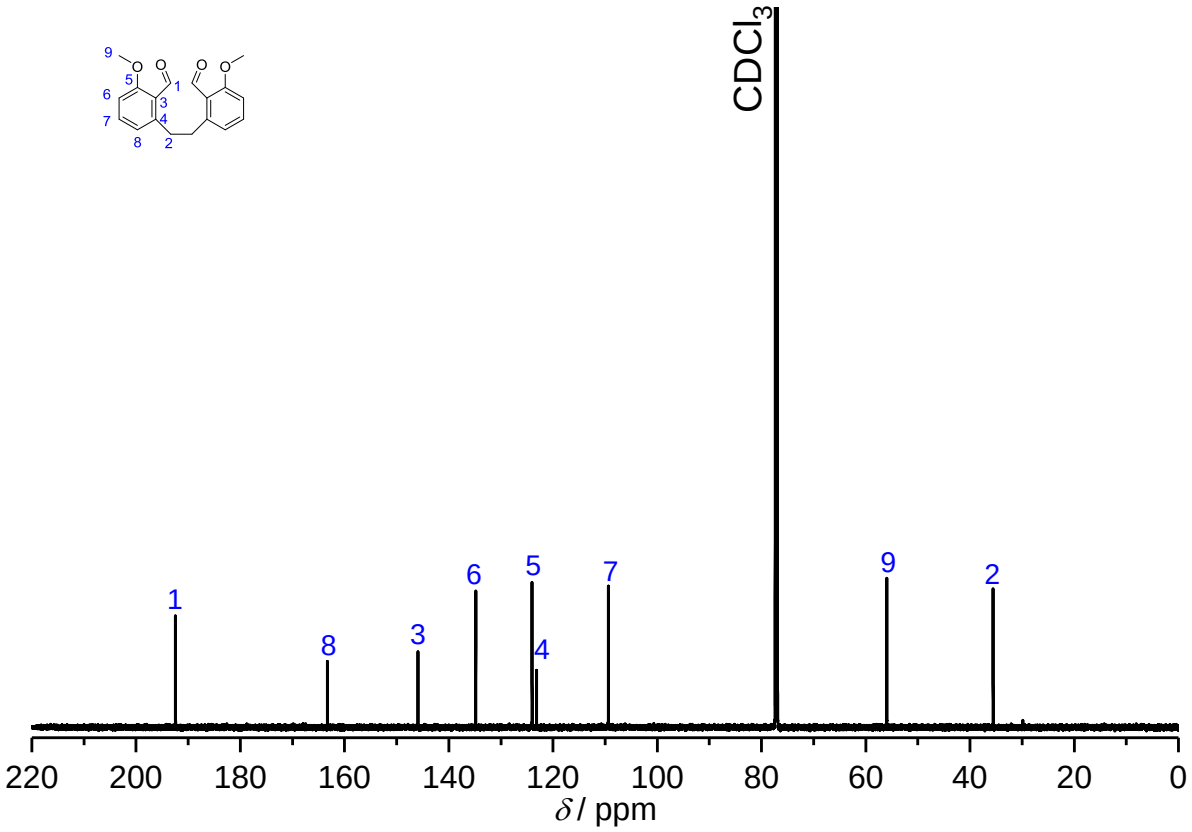

Fig. S10: ^{13}C NMR spectrum of 6,6'-(ethane-1,2-diyl)bis(2-methoxybenzaldehyde) (**[4+4]$_3$**) in $CDCl_3$.

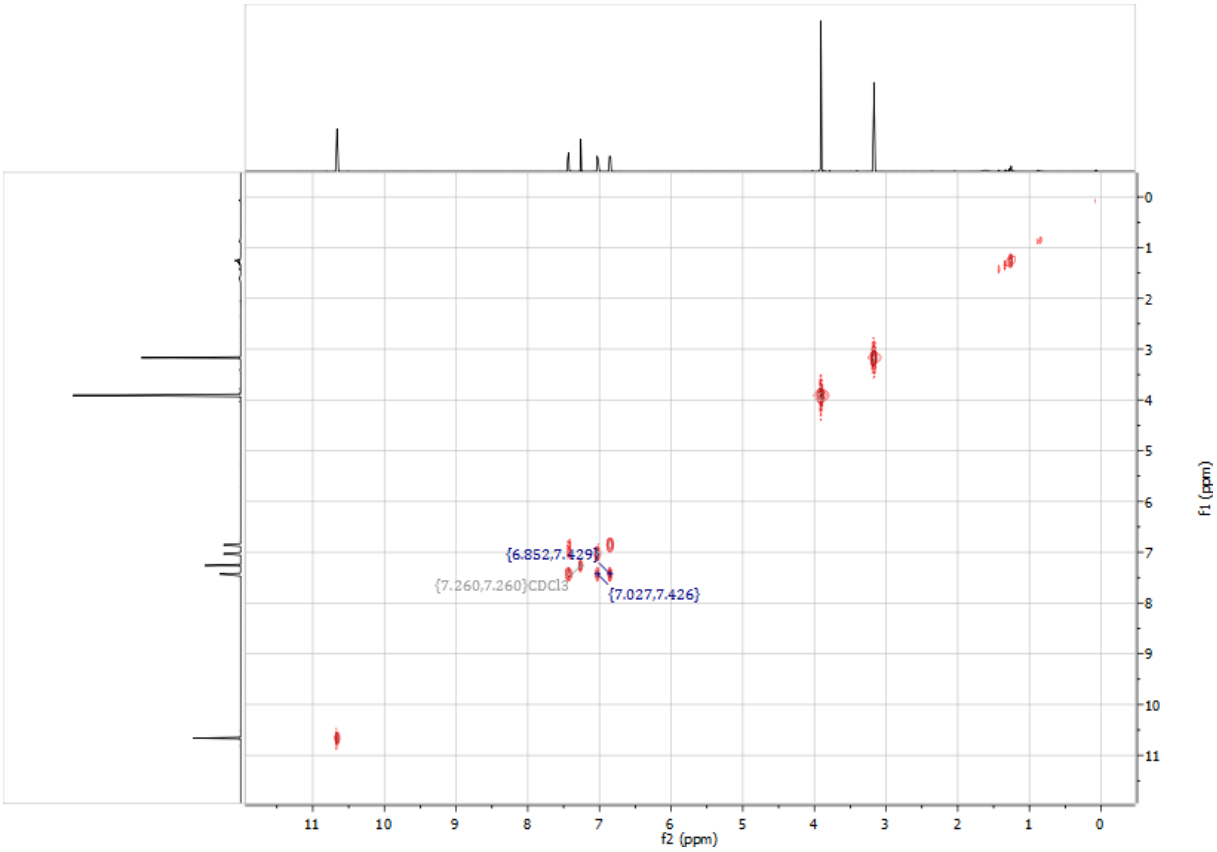

Fig. S11: COSY spectrum of 6,6'-(ethane-1,2-diyl)bis(2-methoxybenzaldehyde) (**[4+4]$_3$**) in $CDCl_3$.

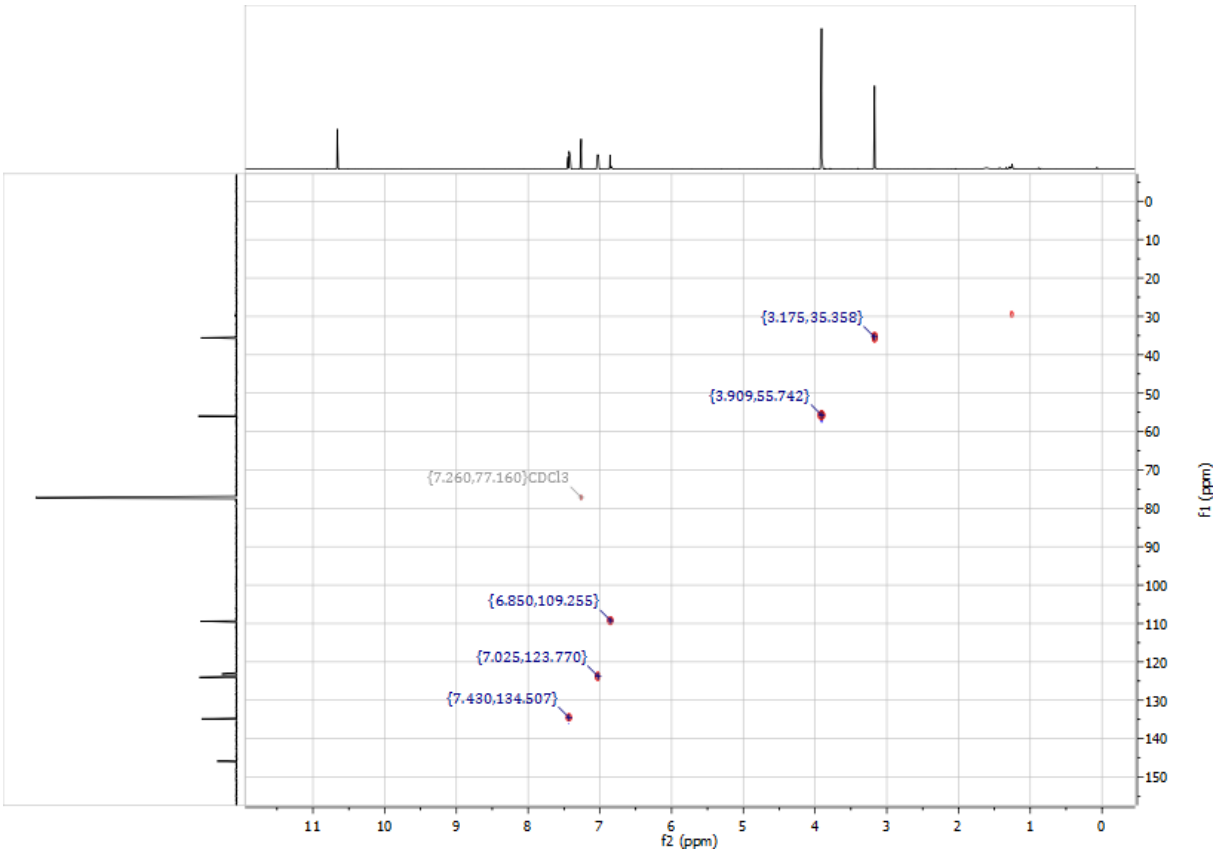

Fig. S12: HSQC spectrum of 6,6'-(ethane-1,2-diyl)bis(2-methoxybenzaldehyde) (**[4+4]$_3$**) in $CDCl_3$.

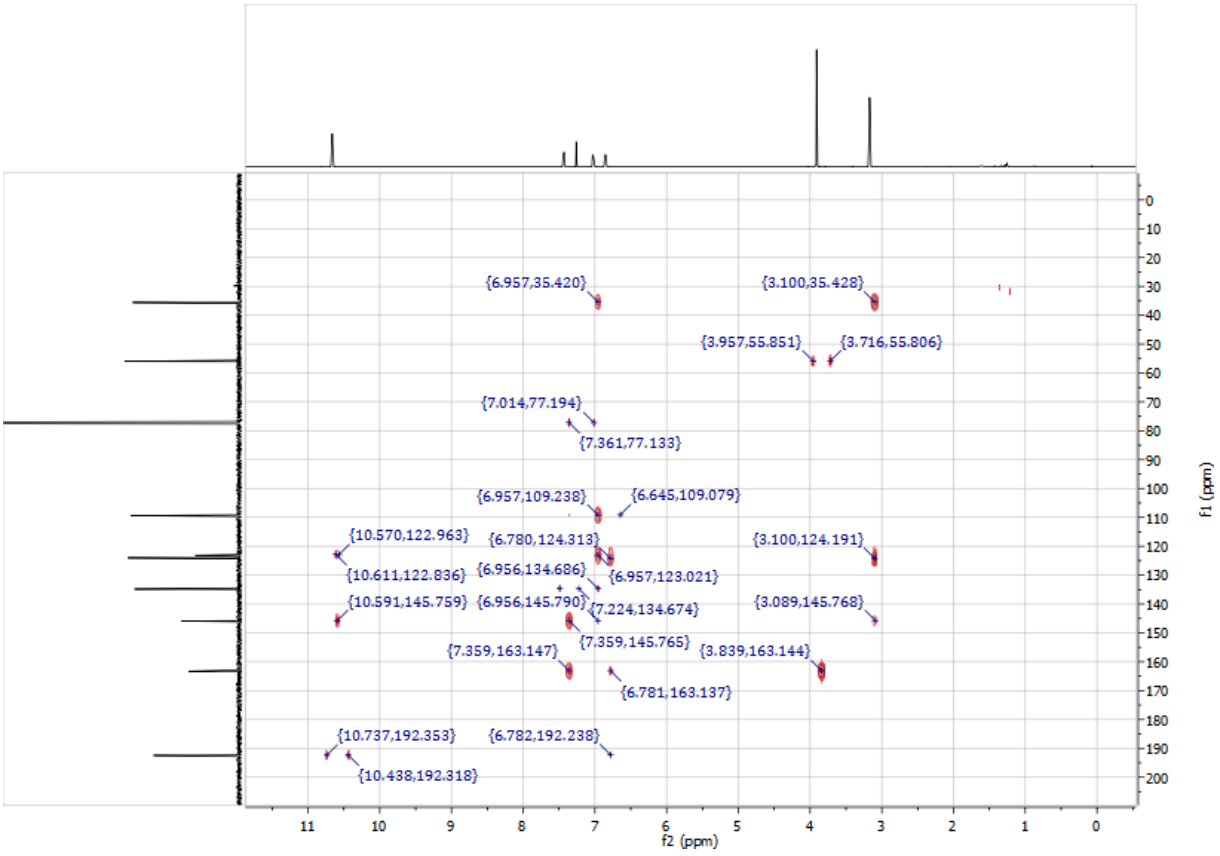

Fig. S13: HMBC spectrum of 6,6'-(ethane-1,2-diyl)bis(2-methoxybenzaldehyde) (**[4+4]$_3$**) in $CDCl_3$.

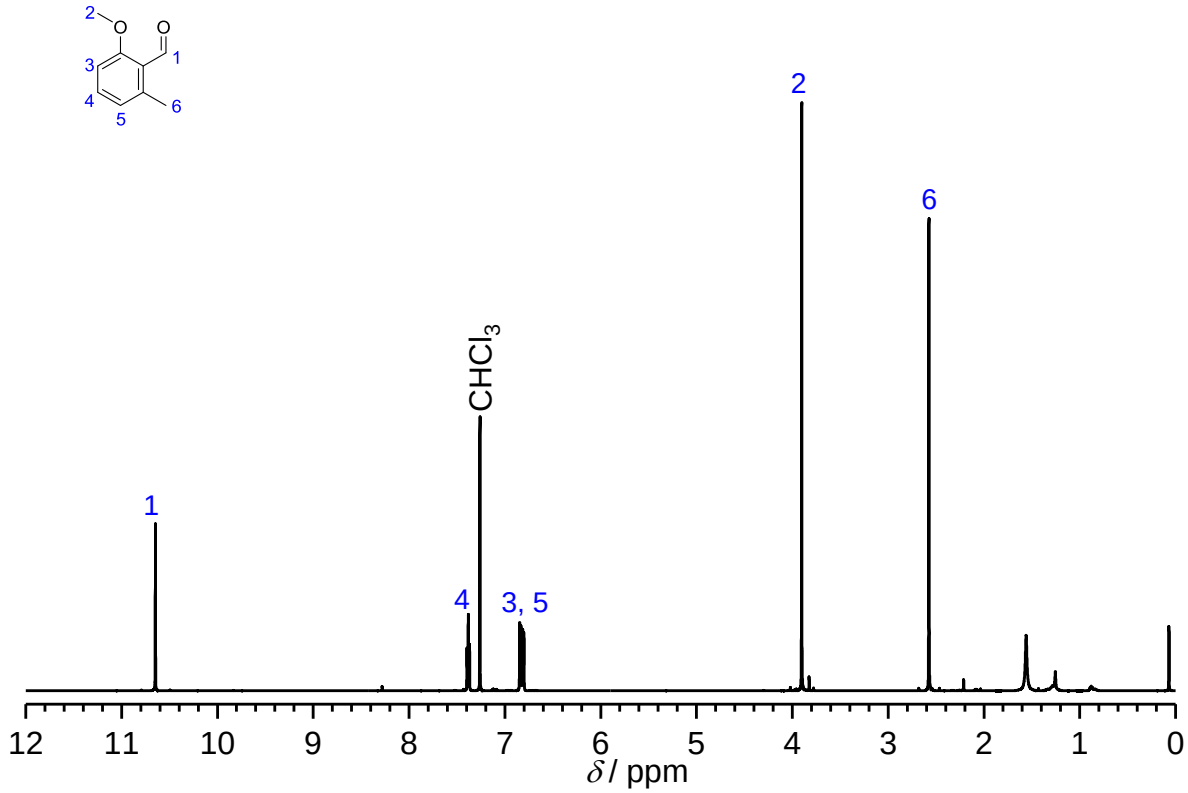

Fig. S14: ^{1}H NMR spectrum of **PE-OMe** in $CDCl_3$.

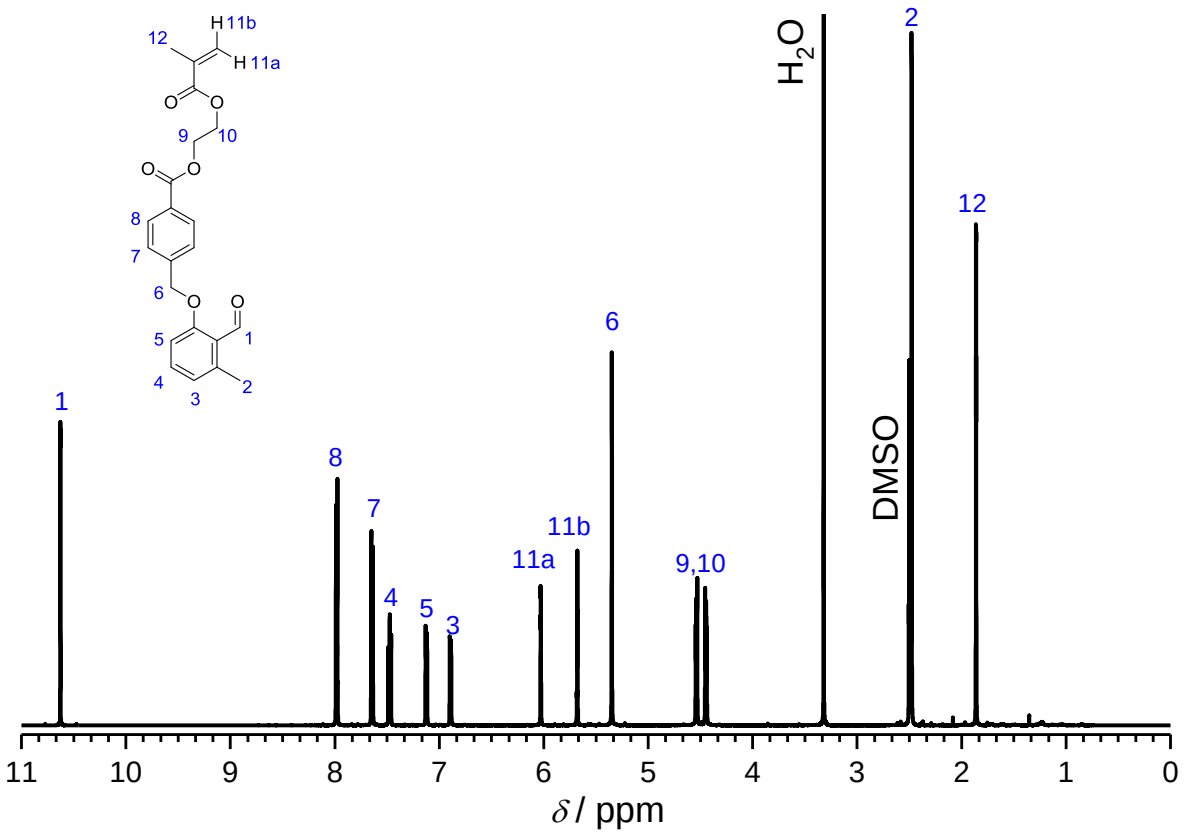

Fig. S15: ^{1}H NMR spectrum of **PEMA** in DMSO-d^{6}.

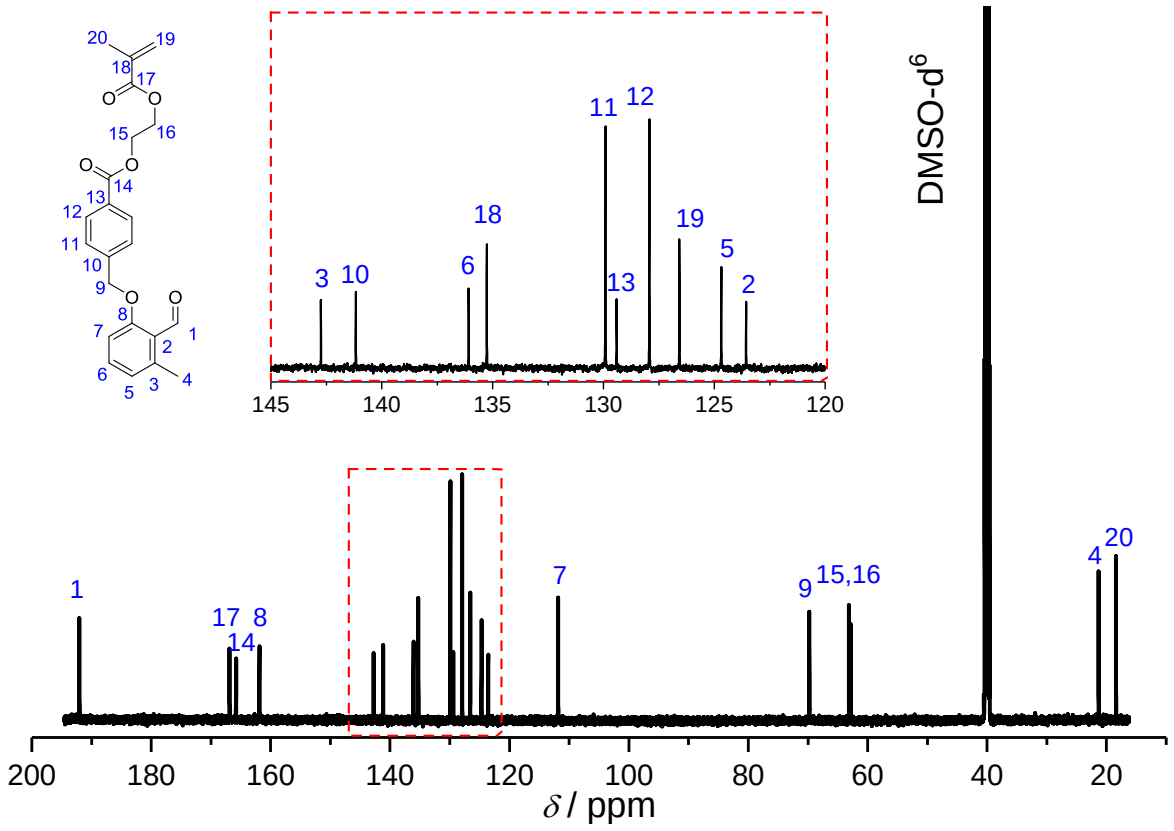

Fig. S16: ^{13}C NMR spectrum of **PEMA** in DMSO-d^{6}.

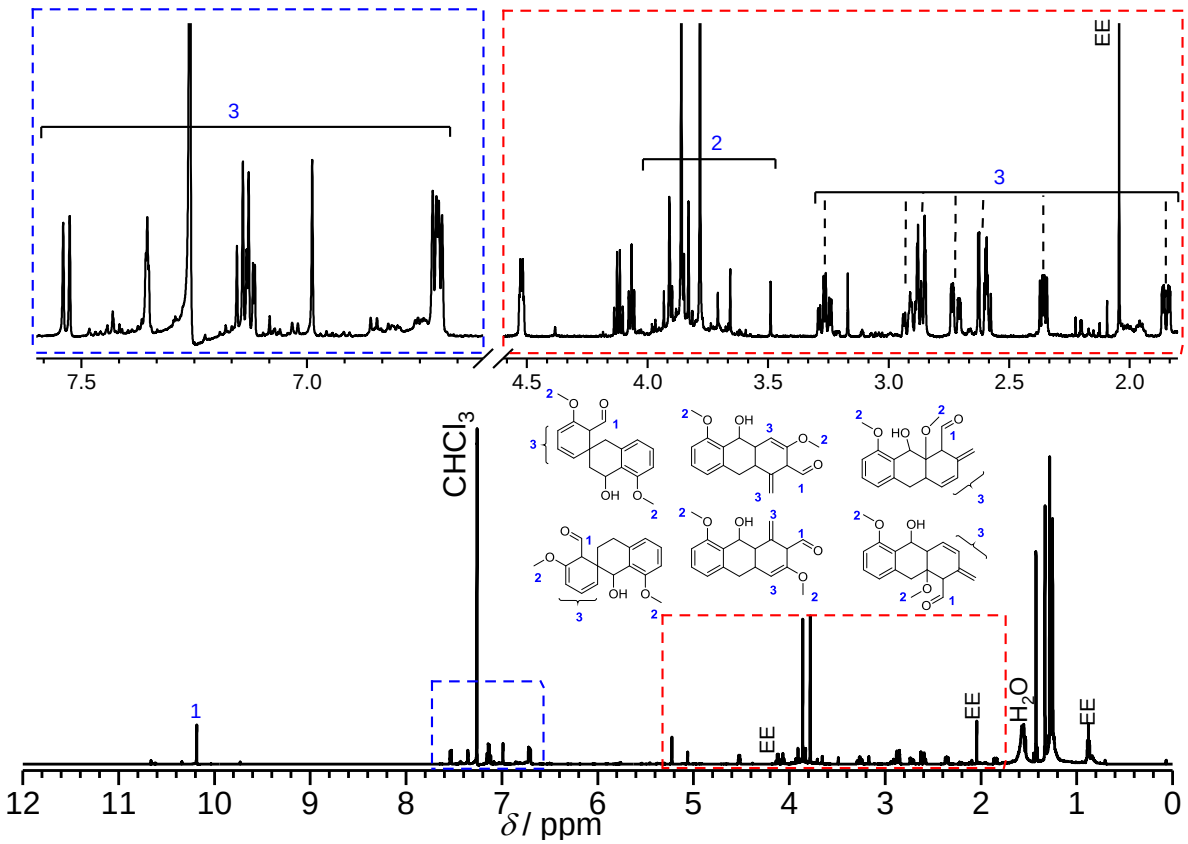

Fig. S17: ^{1}H NMR spectrum of various **[4+2]-cycloadducts** obtained as minor side-products in the preparative photoflow reaction (Section S4.3)

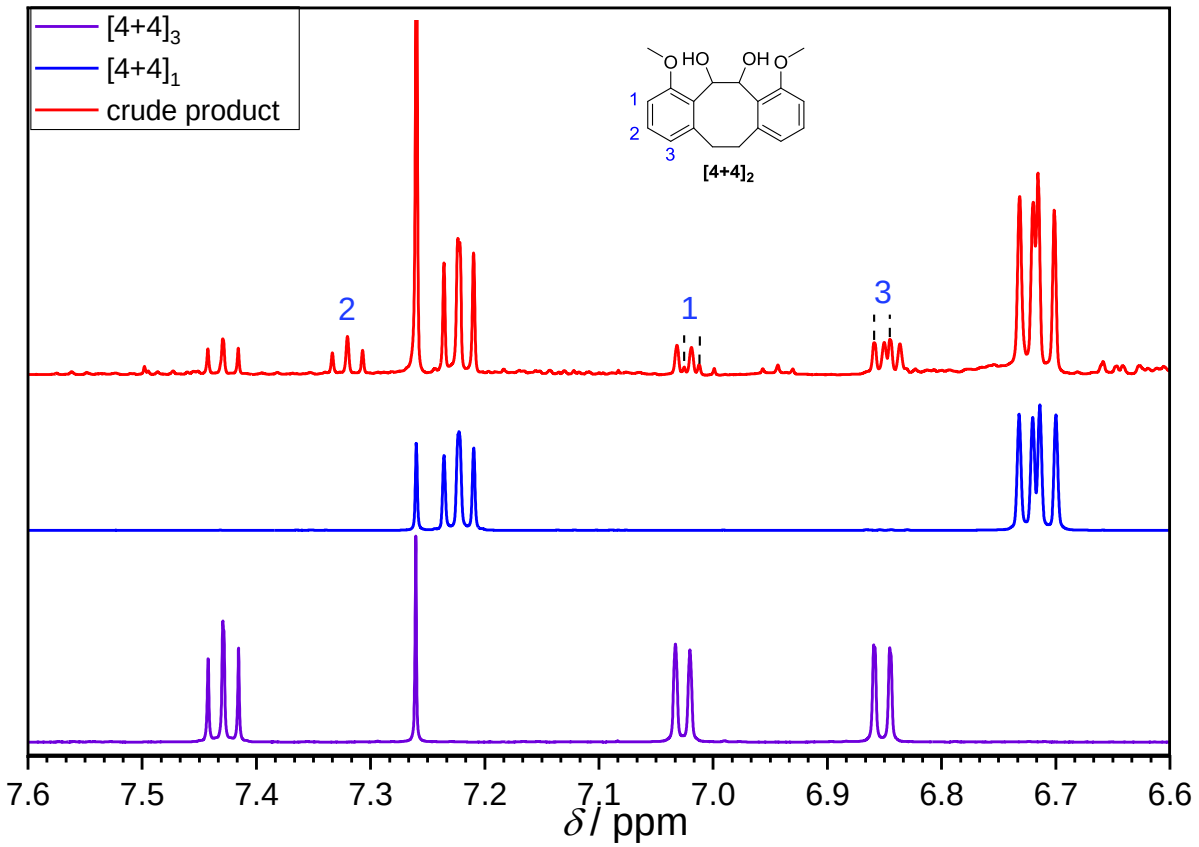

Fig. S18: Aromatic region of the ^{1}H NMR spectra of the crude material obtained in the preparative photoflow reaction (red), the isolated major products **[4+4]$_1$** (blue) and **[4+4]$_3$** (purple). Resonances 1-3 are assigned to the instable vicinal diol **[4+4]$_2$** that was identified in LC-MS (Fig. S31) of the crude material although it could not be isolated afterwards.

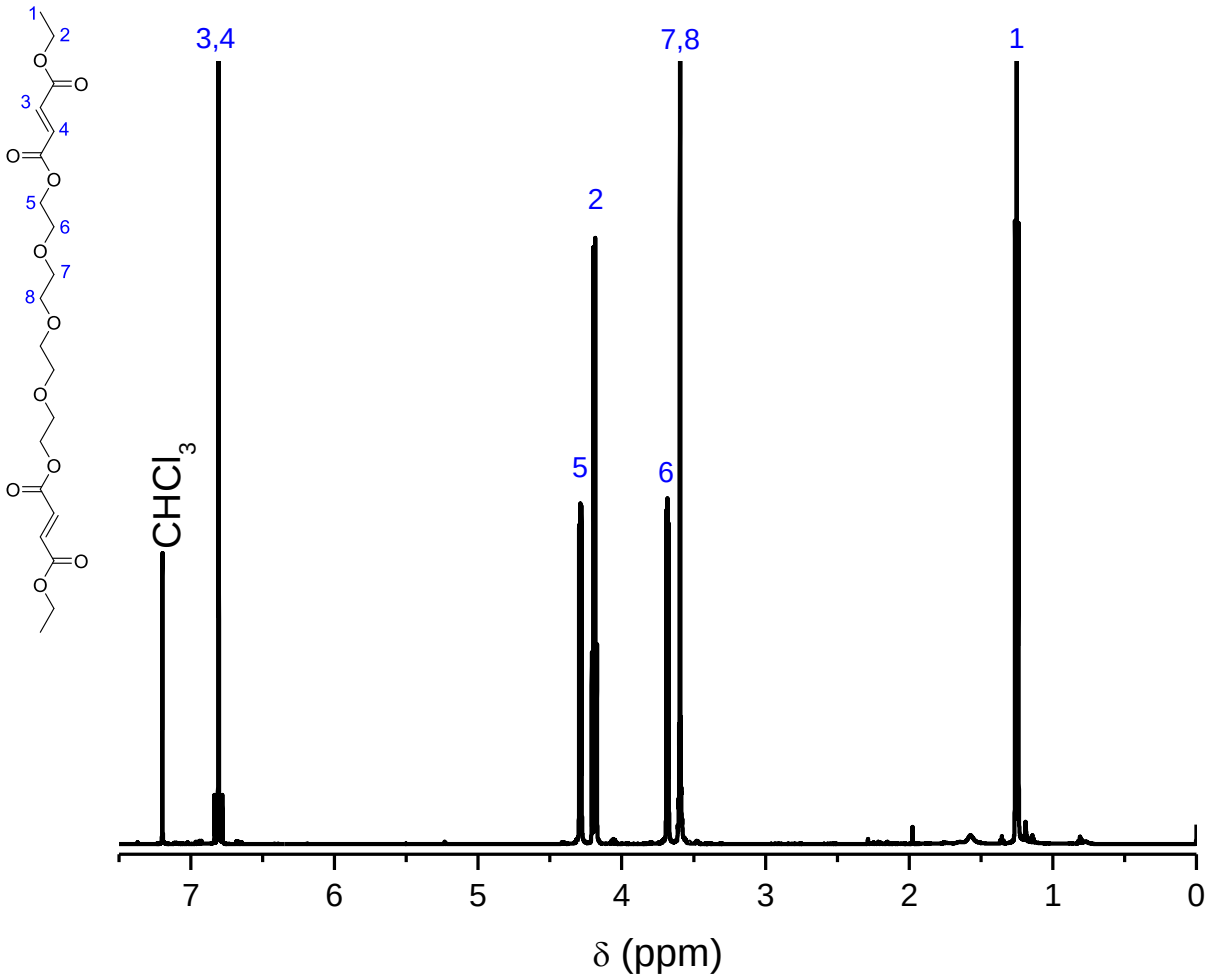

Fig. S19: ^{1}H NMR spectrum of *O,O'*-(((oxybis(ethane-2,1-diyl))bis(oxy))bis(ethane-2,1-diyl)) difumarate in $CDCl_3$.

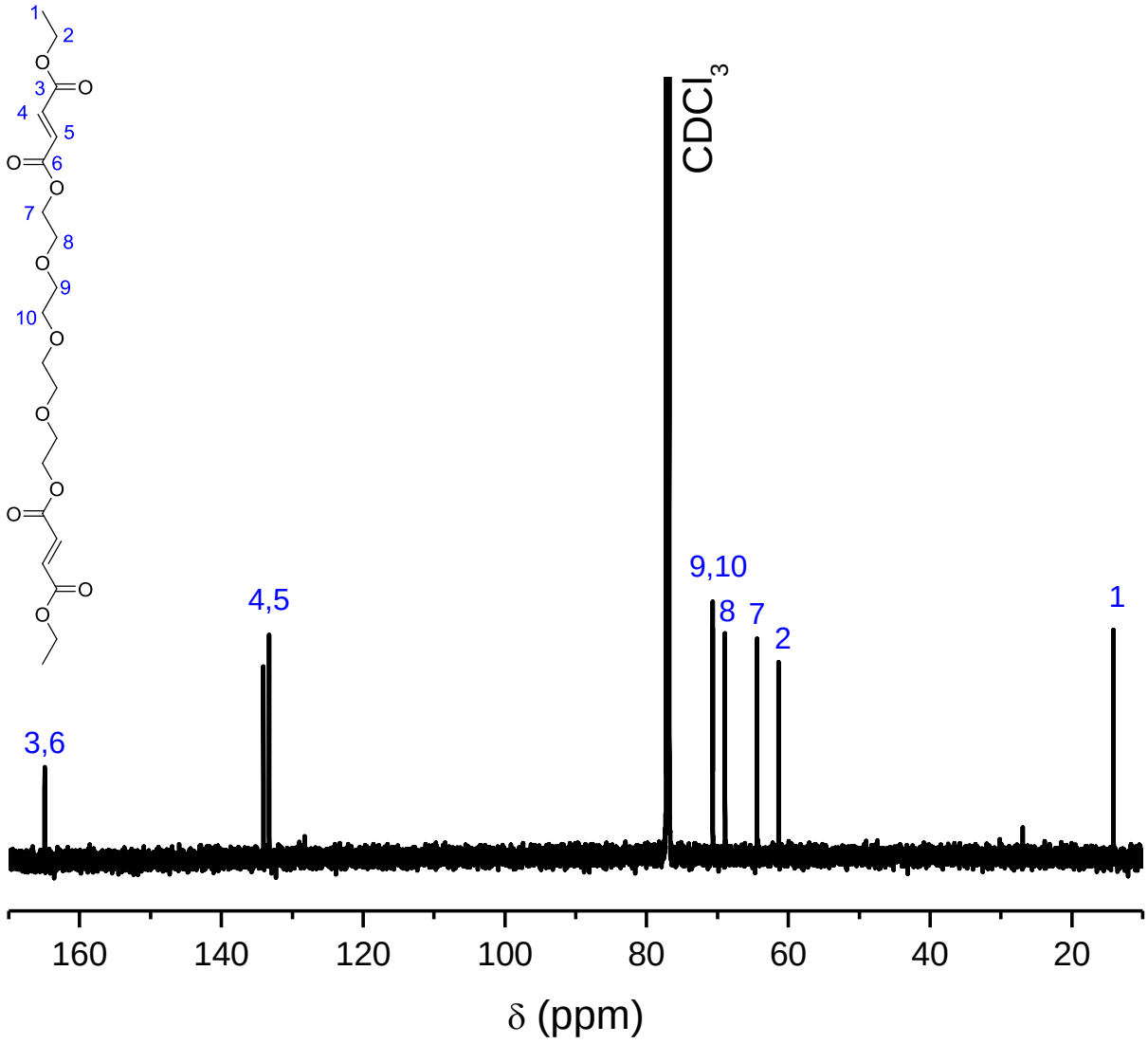

Fig. S20: ^{13}C NMR spectrum of *O,O'*-(((oxybis(ethane-2,1-diyl))bis(oxy))bis(ethane-2,1-diyl)) difumarate in $CDCl_3$.

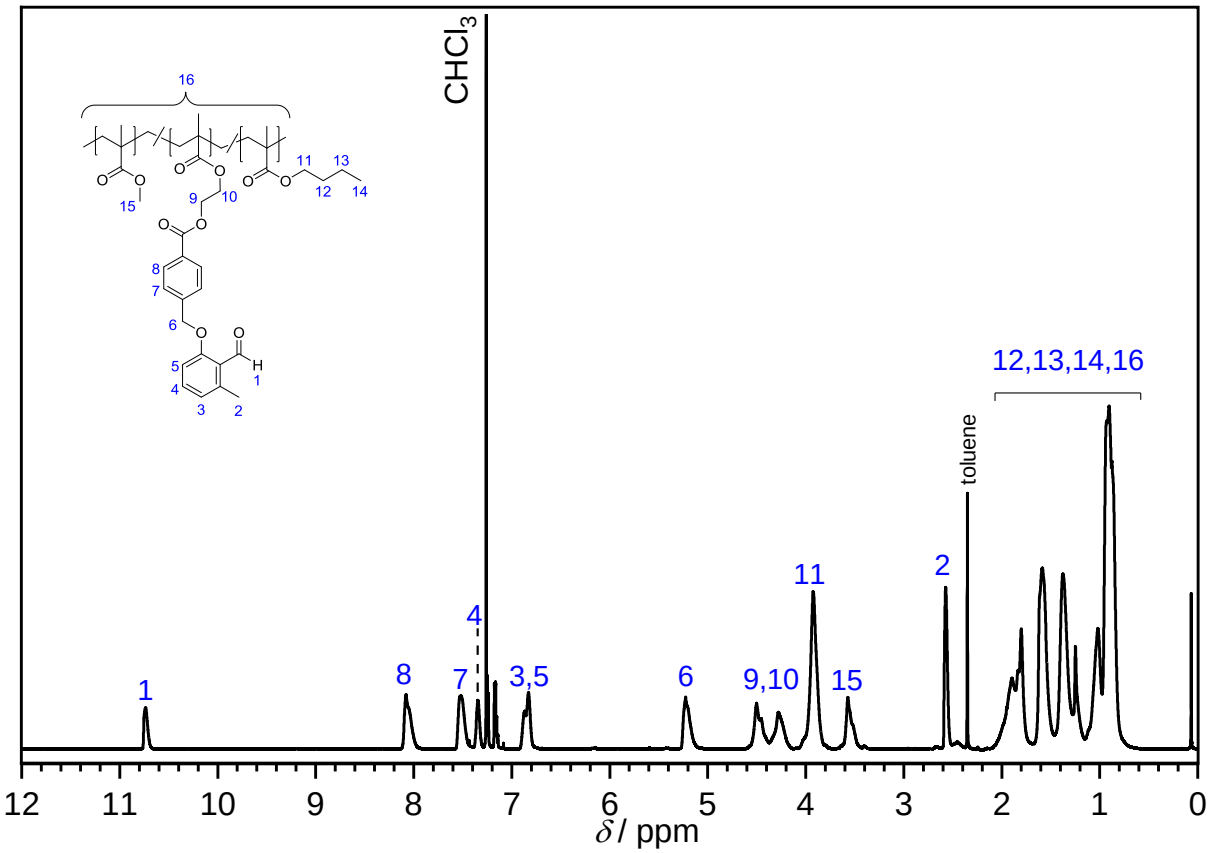

Fig. S21: ^{1}H-NMR spectrum of a copolymer of **p(MMA-co-BMA-co-PEMA)** consisting of 15% MMA, 65% BMA and 20% **PEMA** in $CDCl_3$.

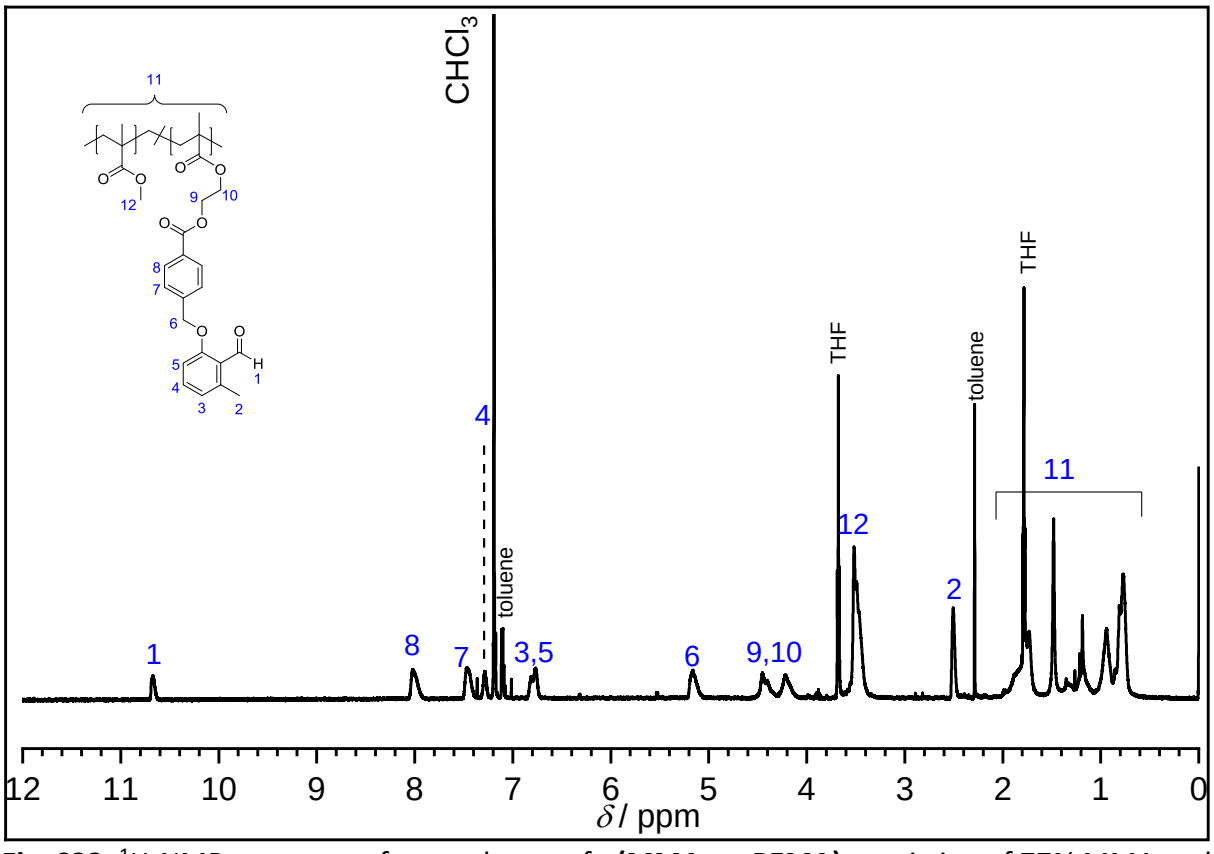

Fig. S22*:* ^{1}H-NMR spectrum of a copolymer of **p(MMA-co-PEMA)** consisting of 77% MMA and 23% **PEMA** in $CDCl_3$.

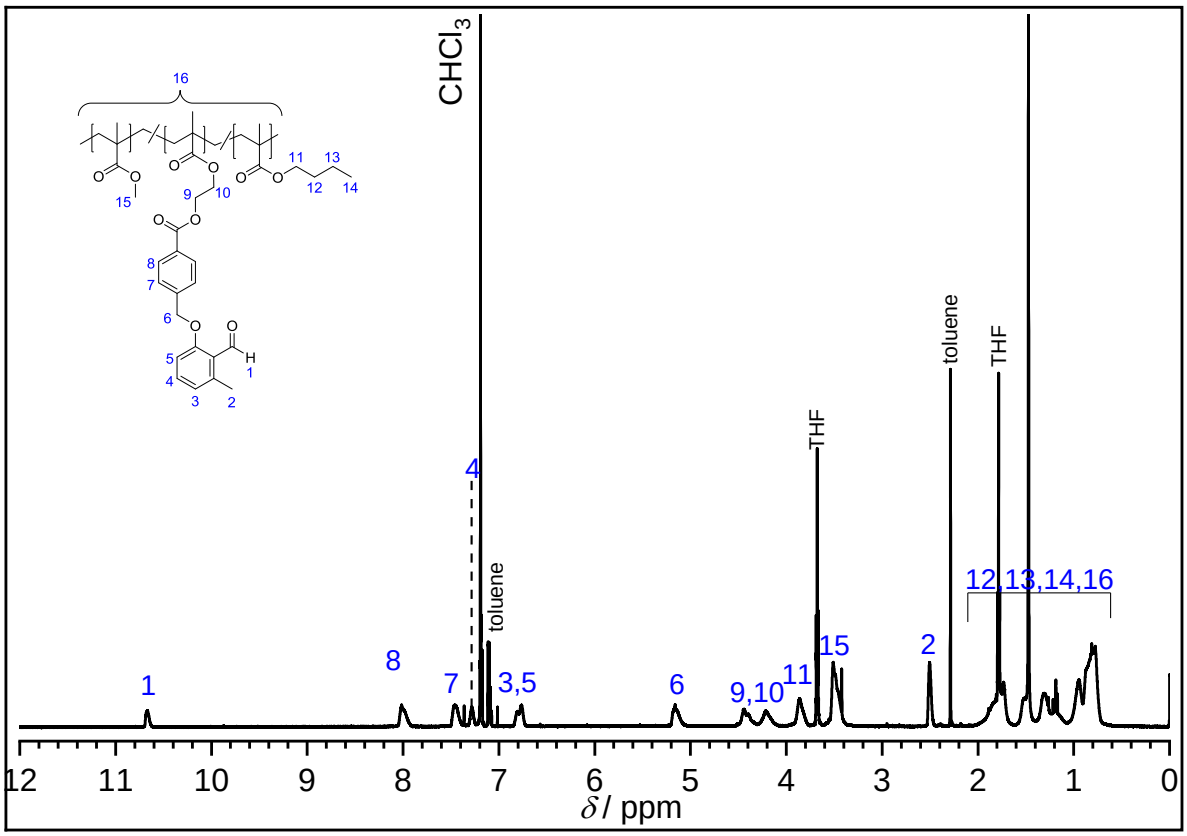

Fig. S23: ^{1}H-NMR spectrum of a copolymer of **p(MMA-co-BMA-co-PEMA)** consisting of 46% MMA, 34% BMA and 20% **PEMA** in $CDCl_3$.

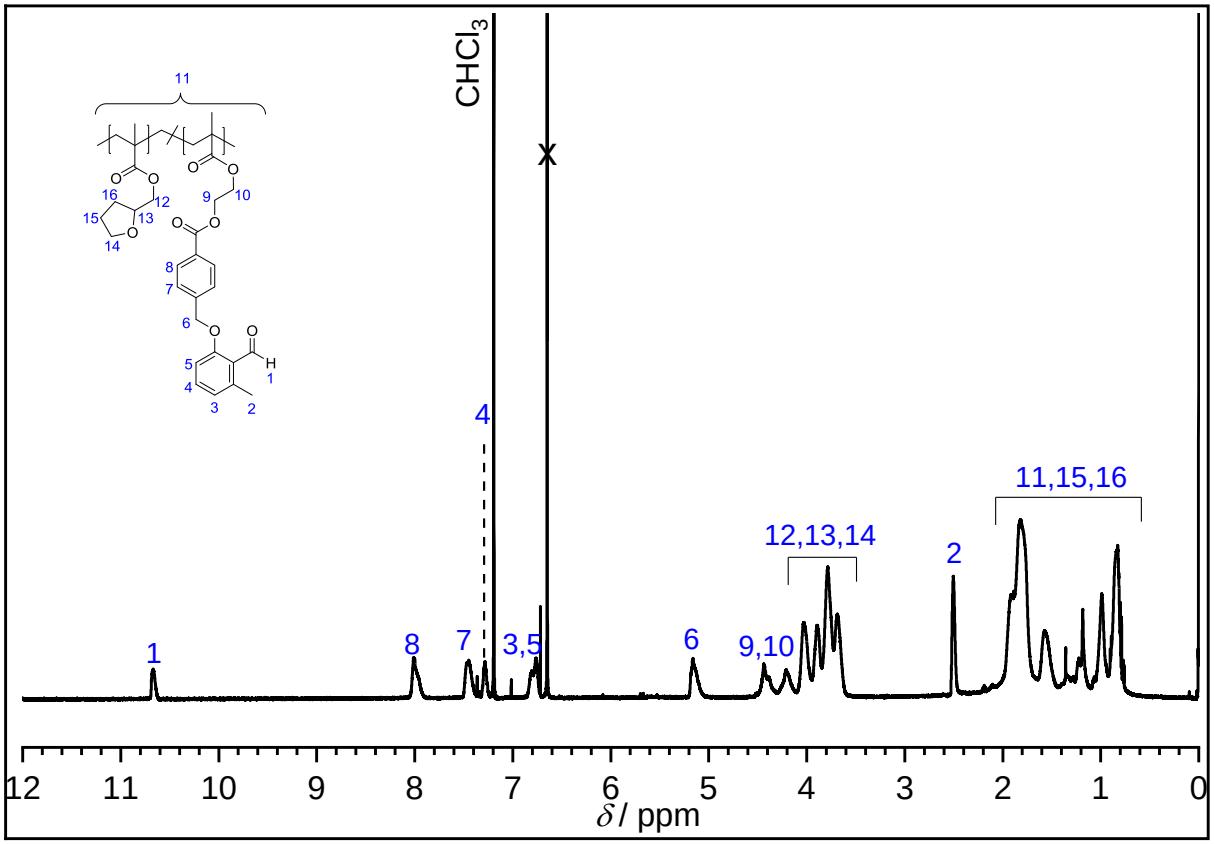

Fig. S24: ^{1}H-NMR spectrum of a copolymer of **p(THFMA-co-PEMA)** consisting of 76% THFMA and 24% **PEMA** in $CDCl_3$.

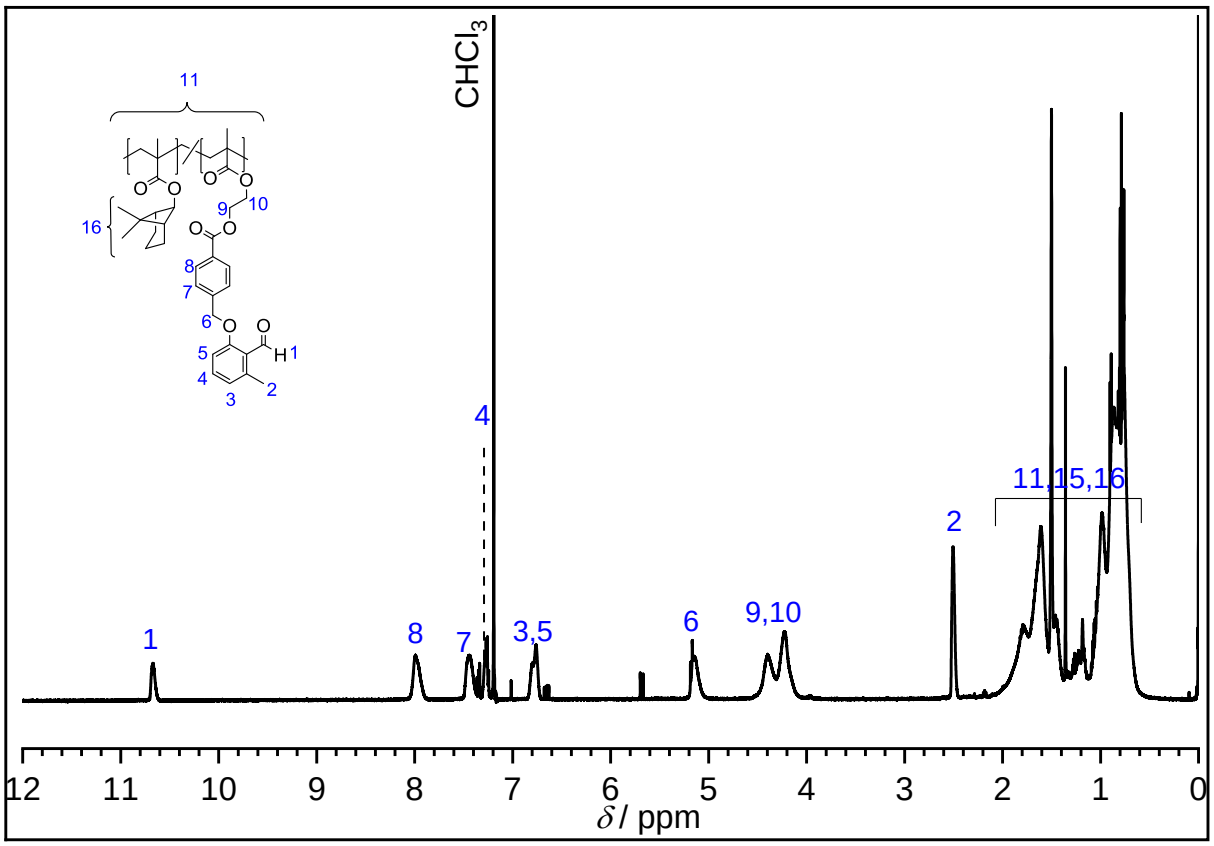

Fig. S25: ^{1}H-NMR spectrum of a copolymer of **p(IBOMA-co-PEMA)** consisting of 80% IBOMA and 20% **PEMA** (feed ratio) in $CDCl_3$.

S6 LC-MS

S6.1 2-methoxy-6-methylbenzaldehyde **(PE-OMe)**

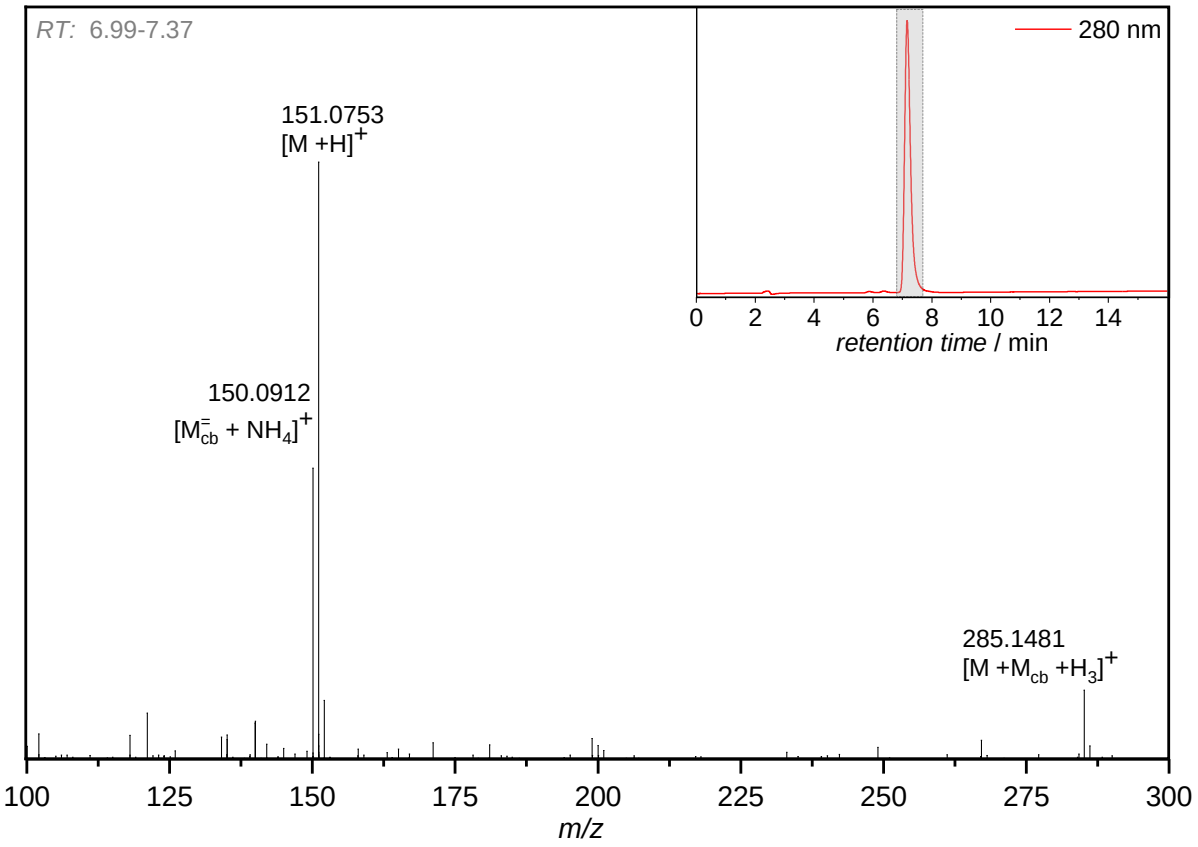

Fig. S26: LC-trace (280 nm detector wavelength) and accumulated mass-spectra of **PE-OMe**.

Table S1*:* Collation of observed signals in the mass spectrum Fig. S26 and comparison with theoretically expected values for *m/z* for the assigned signals.

Symbol	m/z^{exp}	m/z^{theor}	Δ_{ppm}	composition
$[M^{=}_{cb}+NH_4]^+$	150.0912	150.0913	0.67	$C_9H_{12}NO^+$
$[M+ H]^+$	151.0753	151.0754	0.66	$C_9H_{11}O_2^+$
$[M + M_{cb} +H]^+$	285.1481	285.1485	1.40	$C_{18}H_21O_3^+$

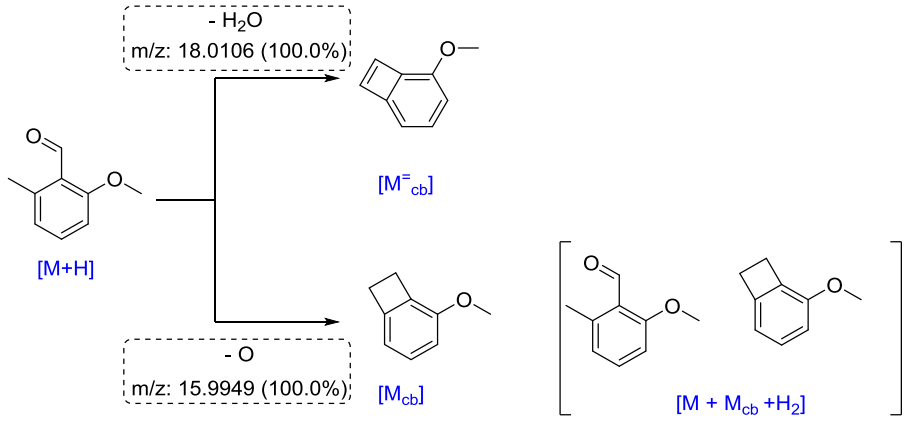

Scheme S2: MS-fragmentation mechanism of **PE-OMe** leading to signals in mass spectrum Fig. S26.

S6.2 4,10-dimethoxy-5,6,11,12-tetrahydrodibenzo[*a,e*][8]annulene-5,11-diol (**[4+4]$_1$**)

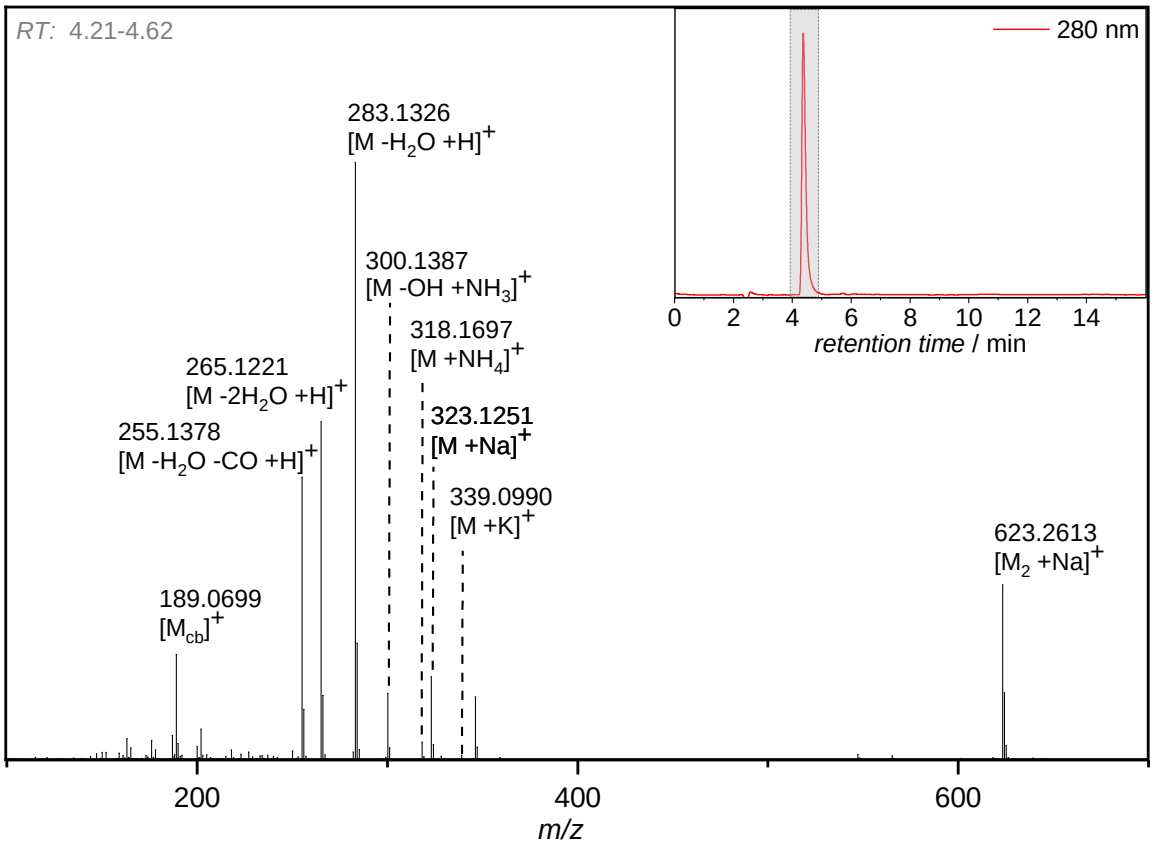

Fig. S27 LC-trace (280 nm detector wavelength) and accumulated mass-spectra of **[4+4]$_1$**.

Table S2: Collation of observed signals in the mass spectrum Fig. S27 and comparison with theoretically expected *m/z* values for the assigned signals.

symbol	m/z^{exp}	m/z^{theor}	Δ_{ppm}	composition
$[M_{cb} + H]^+$	189.0698	189.0699	0.53	$C_{15}H_9^+$
$[M -H_2O -CO +H]^+$	255.1378	255.1380	0.78	$C_{17}H_{19}O_2^+$
$[M -2\ H_2O +H]^+$	265.1221	265.1223	0.75	$C_{18}H_{17}O_2^+$
$[M -H_2O +H]^+$	283.1326	283.1329	1.06	$C_{18}H_{19}O_3^+$
$[M -OH +NH_3]^+$	300.1591	300.1594	1.00	$C_{18}H_{22}NO_3^+$
$[M +NH_4]^+$	318.1697	318.17	0.94	$C_{18}H_{24}NO_4^+$
$[M +Na]^+$	323.1251	323.1254	0.93	$C_{18}H_{20}NaO_4^+$
$[M +K]^+$	339.099	339.0993	0.88	$C_{18}H_{20}KO_4^+$
$[M_2 +Na]^+$	623.2613	623.2615	0.32	$C_{36}H_{40}NaO_8^+$

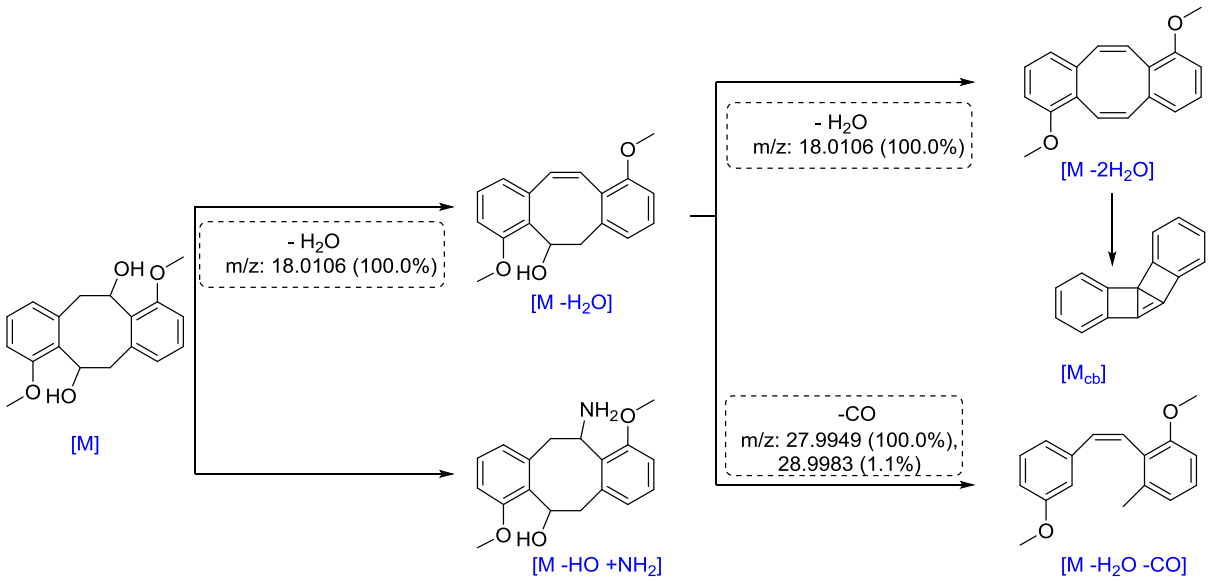

Scheme S3: MS-fragmentation mechanism of **$[4+4]_1$** leading to signals in mass spectrum Fig. S27.

S6.3 6,6'-(ethane-1,2-diyl)bis(2-methoxybenzaldehyde) (**[4+4]$_3$**)

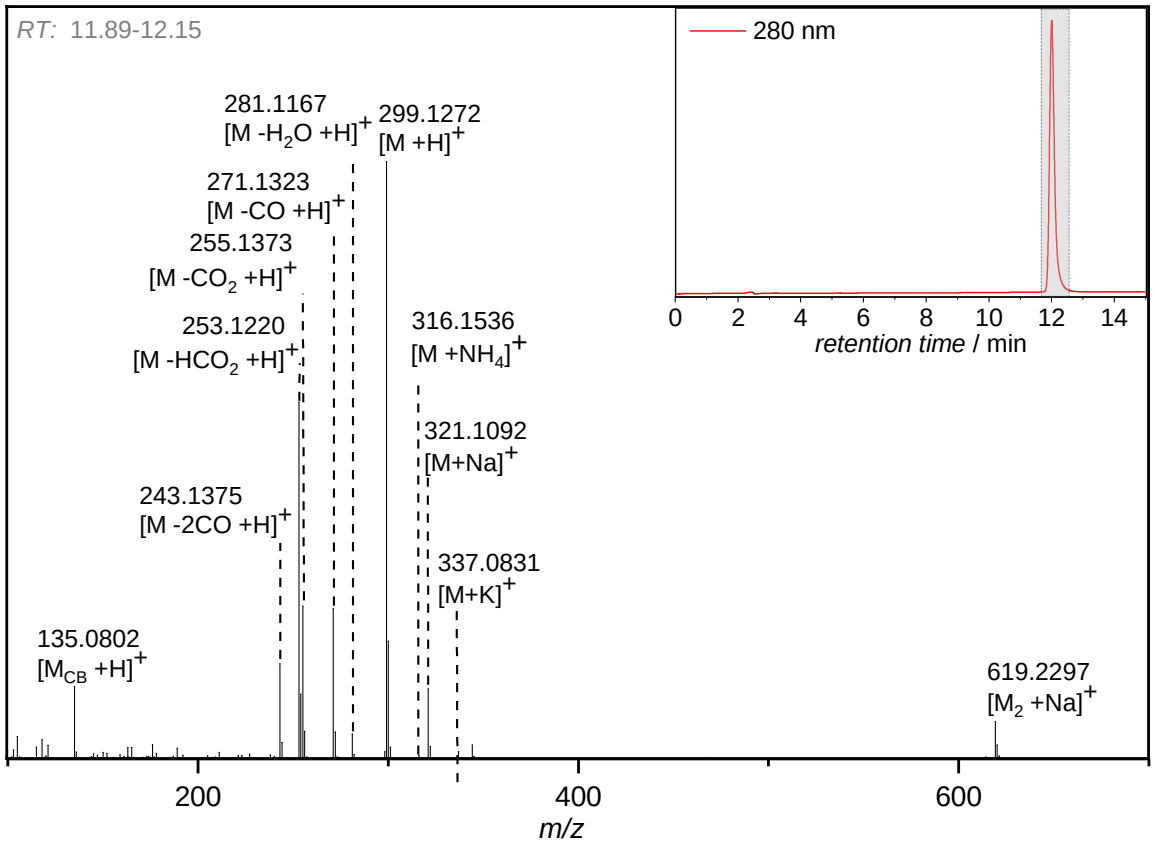

Fig. S28: LC-trace (280 nm detector wavelength) and accumulated mass-spectra of **[4+4]$_3$**.

Table S3: Collation of observed signals in the mass spectrum Fig. S28 and comparison with theoretically expected *m/z* values for the assigned signals.

symbol	m/z^{exp}	m/z^{theor}	Δ_{ppm}	composition
$[M_{cb} +H]^+$	135.0802	135.0804	1.48	$C_9H_{11}O^+$
$[M -2CO +H]^+$	243.1375	243.1380	2.06	$C_{16}H_{19}O_2^+$
$[M -HCO_2H +H]^+$	253.122	253.1223	1.19	$C_{17}H_{17}O_2^+$
$[M -CO_2 +H]^+$	255.1373	255.138	2.74	$C_{17}H_{19}O_2^+$
$[M -CO +H]^+$	271.1323	271.1329	2.21	$C_{17}H_{19}O_3^+$
$[M -H_2O +H]^+$	281.1167	281.1172	1.78	$C_{18}H_{17}O_3^+$
$[M+H]^+$	299.1272	299.1278	2.01	$C_{18}H_{19}O_4^+$
$[M+NH_4]^+$	316.1536	316.1543	2.21	$C_{18}H_{22}NO_4^+$
$[M +Na]^+$	321.1092	321.1097	1.56	$C_{18}H_{18}NaO_4^+$
$[M +K]^+$	337.0831	337.0837	1.78	$C_{18}H_{18}KO_4^+$
$[M_2 +Na]^+$	619.2297	619.2302	0.81	$C_{36}H_{36}NaO_8^+$

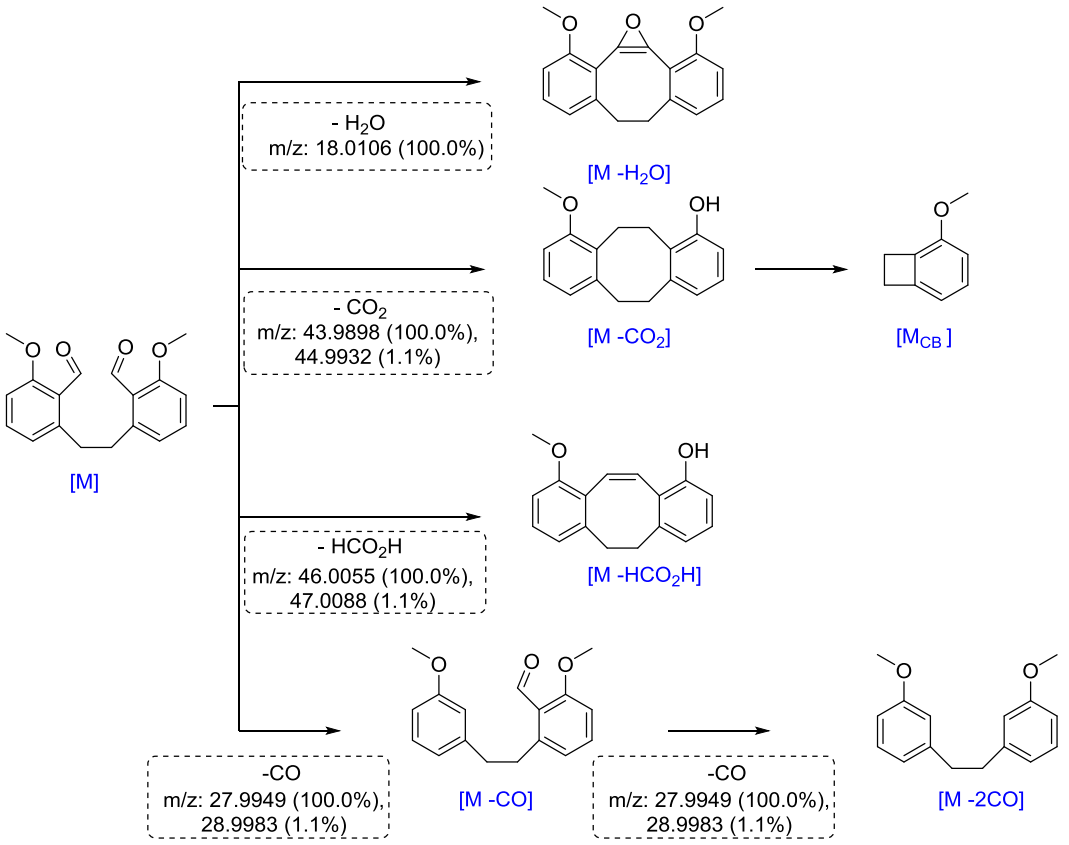

Scheme S3: MS-fragmentation mechanism of (**[4+4]$_3$**) leading to signals in mass spectrum Fig. S28.

S6.4 LC-analysis of the photoinduced dimerization of **PE-OMe**.

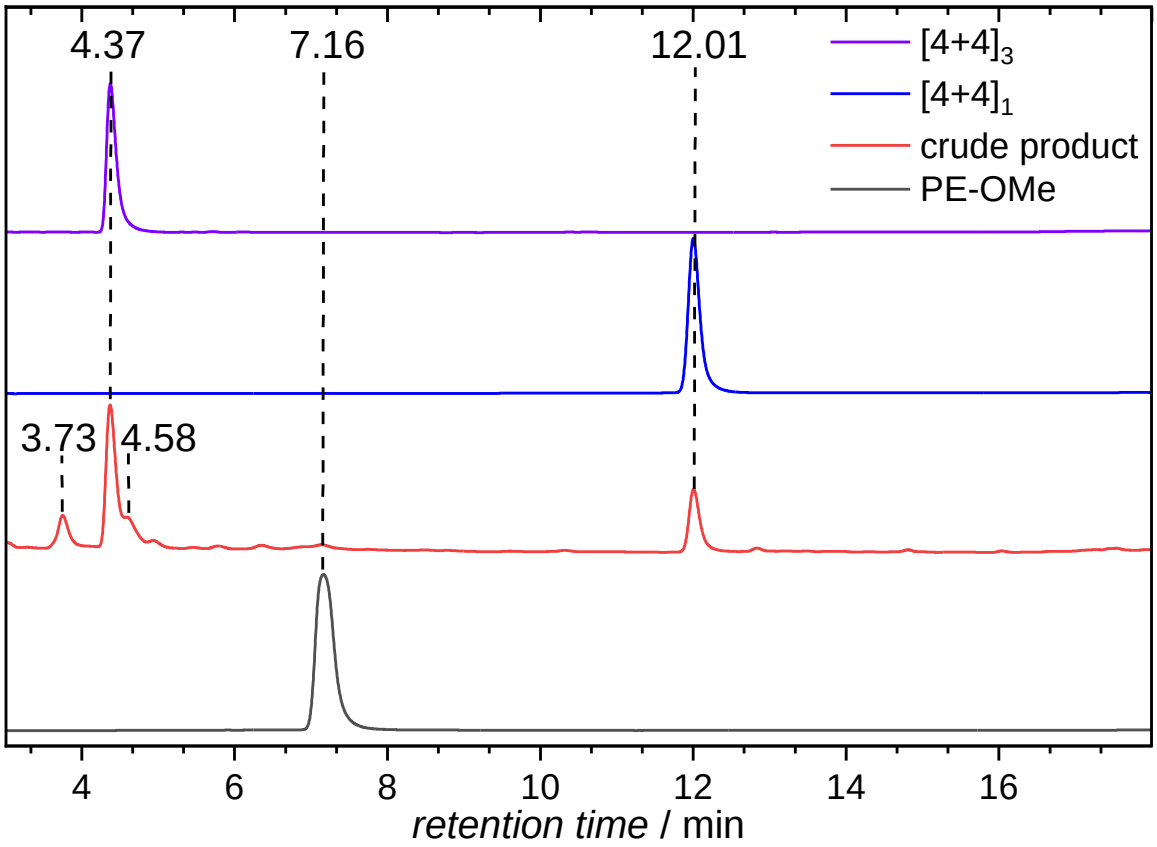

Fig. S29: LC-traces (280 nm) of **PE-OMe** (black), the crude product (red) obtained in the preparative photoflow reaction. (Section S4.3) and the isolated main products **[4+4]$_1$** (blue) and **[4+4]$_3$** (violet).

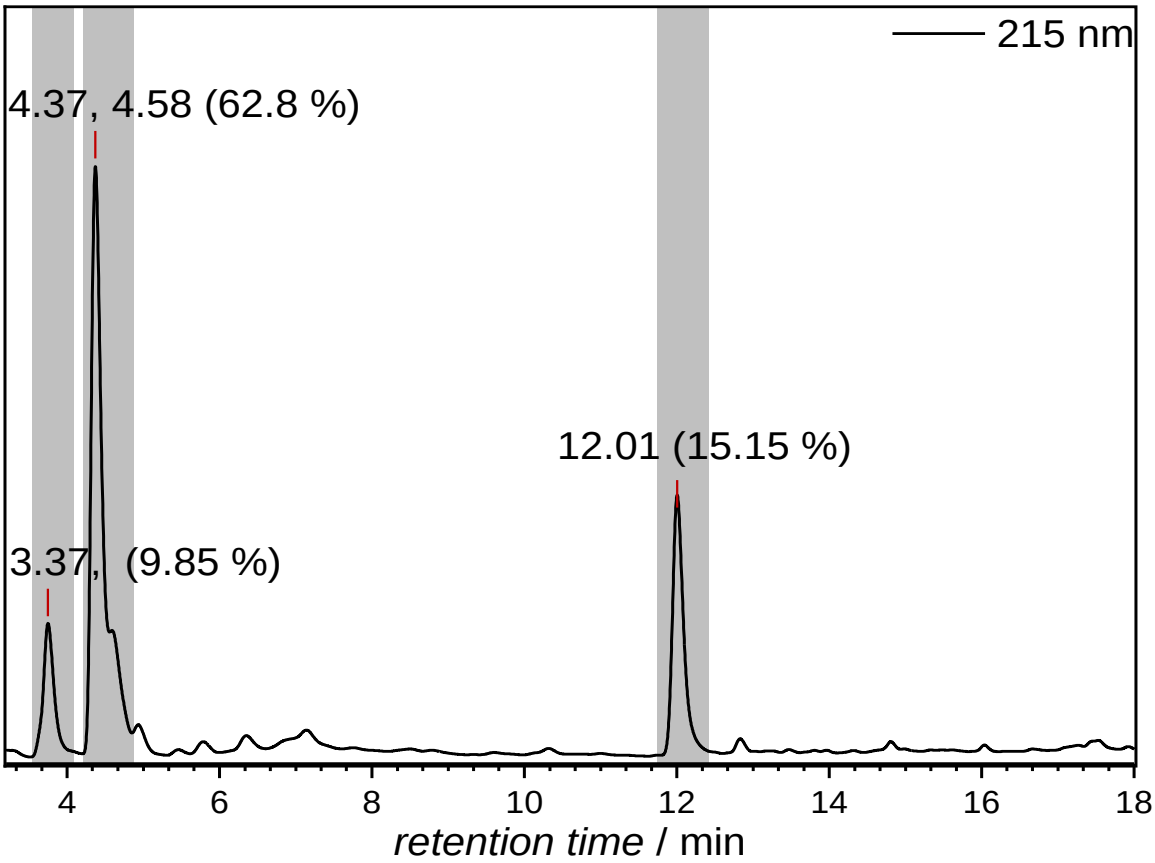

Fig. S30: LC-trace (280 nm) the crude product obtained in the preparative photoflow reaction. (Section S4.3). Integration of main product peaks **[4+4]$_1$**, **[4+4]$_2$**, **[4+4]$_3$** and corresponding peak area.

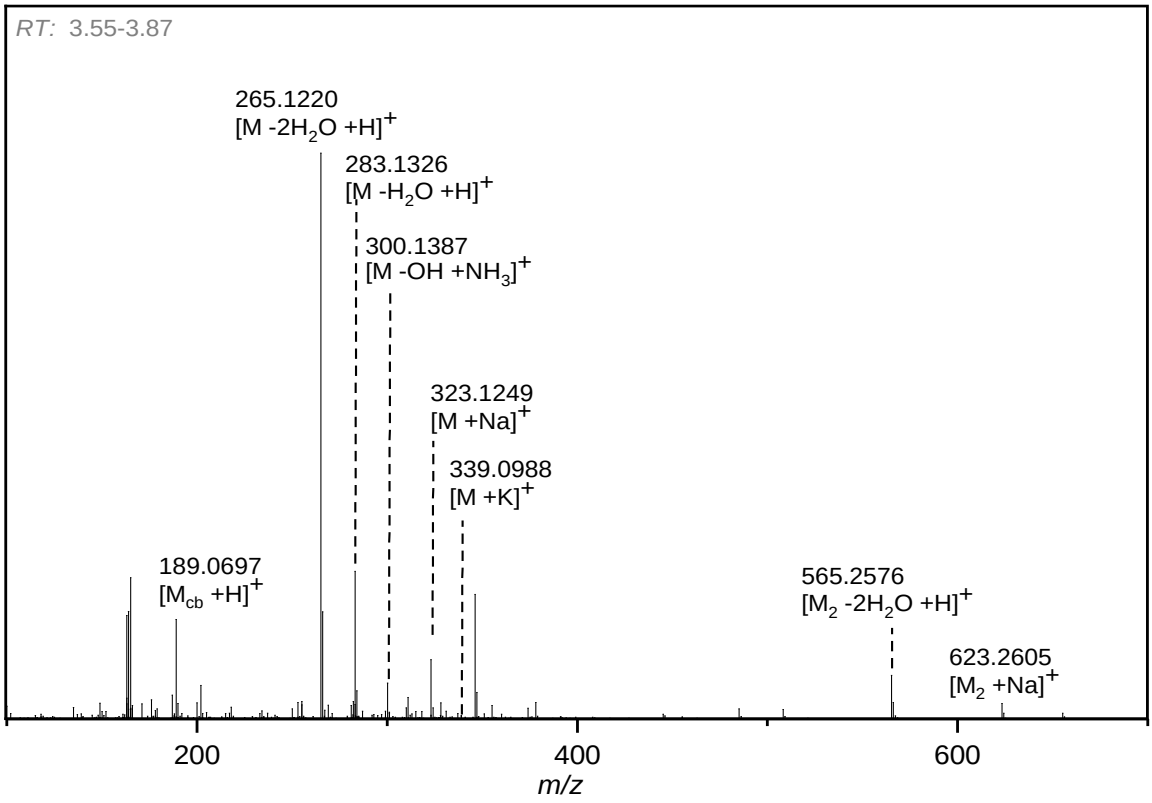

Fig. S31: Accumulated mass-spectra of 4,7-dimethoxy-5,6,11,12-tetrahydro-dibenzo[*a,e*][8]annulene-5,6-diol **[4+4]$_2$** obtained from crude LC trace in Fig. S30.

Table S4: Collation of observed signals in the mass spectrum Fig. S31 and comparison with theoretically expected *m/z* values for the assigned signals.

symbol	m/z^{exp}	m/z^{theor}	Δ_{ppm}	composition
$[M_{CB}+H]^+$	189.0697	189.0699	1.06	$C_{15}H_9^+$
$[M-2H_2O+H]^+$	265.122	265.1223	1.13	$C_{18}H_{17}O_2^+$
$[M-H_2O+H]^+$	283.1326	283.1329	1.06	$C_{18}H_{19}O_3^+$
$[M-OH+NH_3]^+$	300.1590	300.1594	1.33	$C_{18}H_{22}NO_3^+$
$[M+Na]^+$	323.1249	323.1254	1.55	$C_{18}H_{20}NaO_4^+$
$[M+K]^+$	339.0988	339.0993	1.47	$C_{18}H_{20}KO_4^+$
$[M_2-2H_2O+H]^+$	565.2576	565.2585	1.59	$C_{36}H_{37}O_6^+$
$[M_2+Na]^+$	623.2605	623.2615	1.60	$C_{36}H_{40}NaO_8^+$

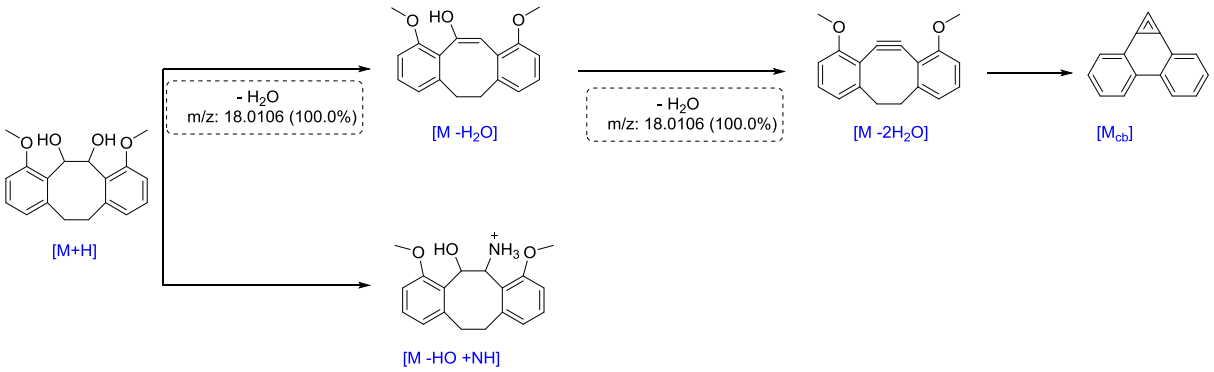

Scheme S4: MS-fragmentation mechanism of **[4+4]$_2$** leading to signals in mass spectrum Fig. S31.

S7 Size Exclusion Chromatography (SEC)

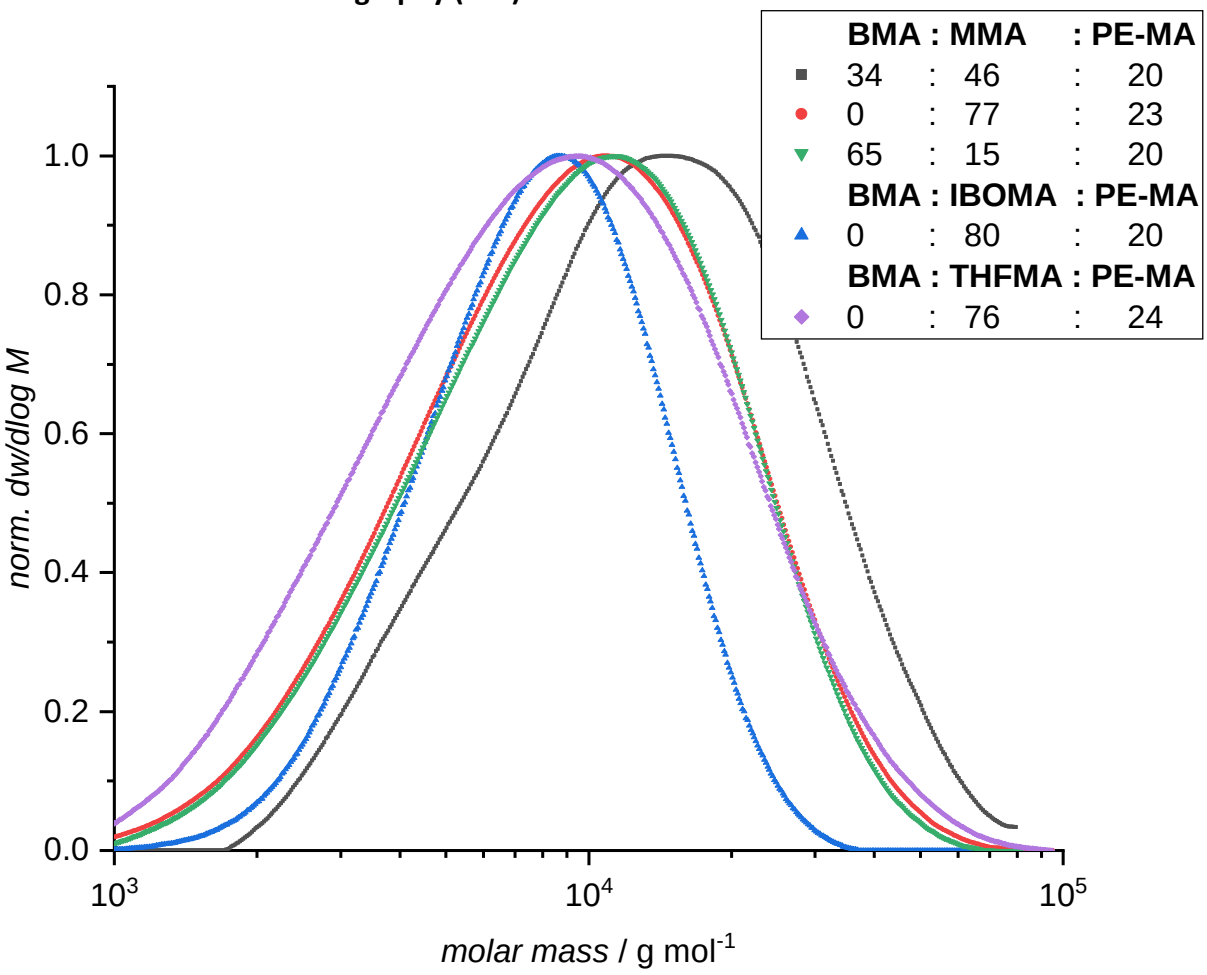

Fig. S32: SEC traces of all polymers in Table 1 (main document).

S8 Differential Scanning Calorimetry (DSC)

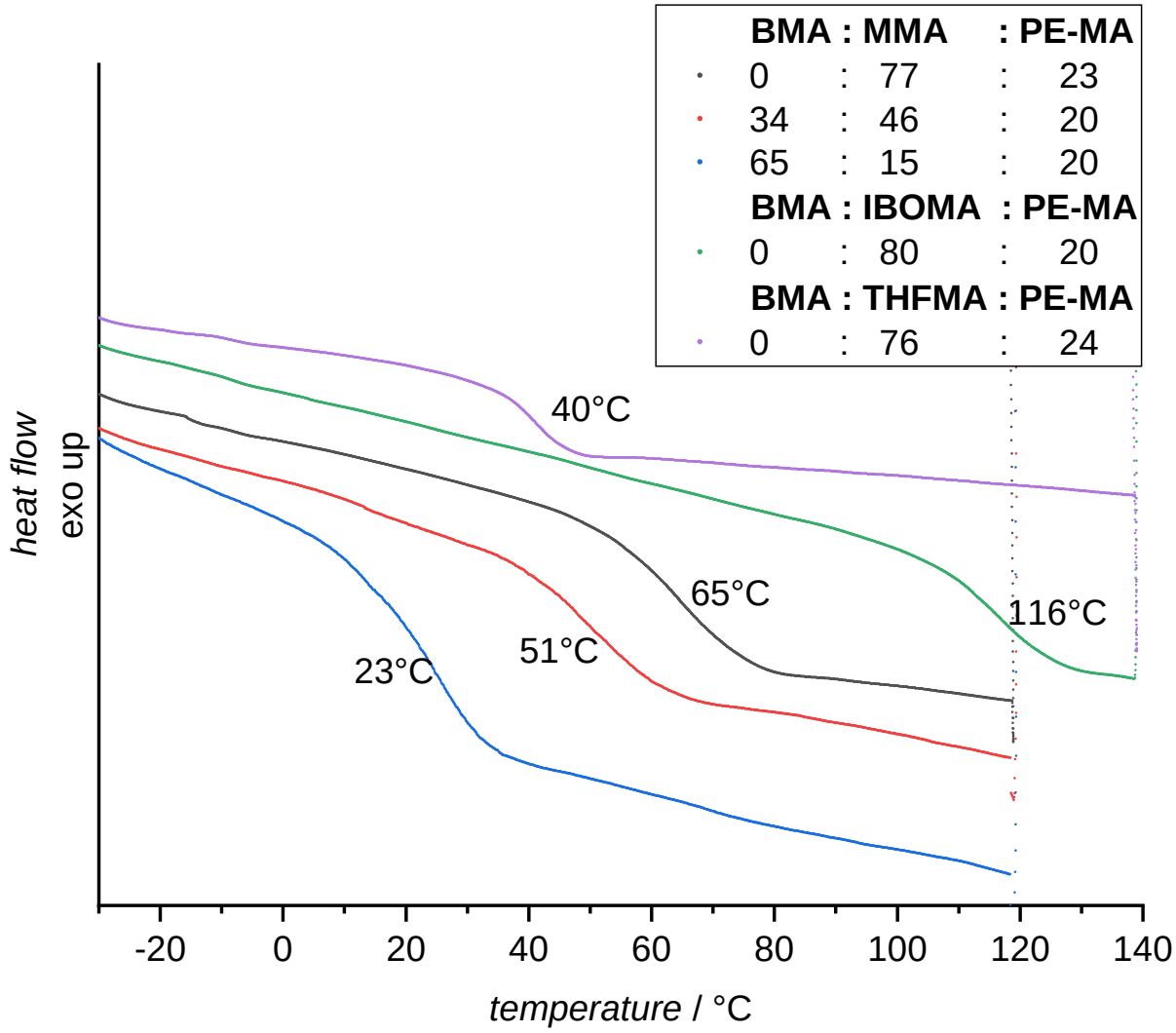

Fig. S33: The second heating step of the DSC results in Table 1 (main document) is depicted, showing all the reported glass transition temperatures.

S9 Thermal Gravimetric Analysis (TGA)

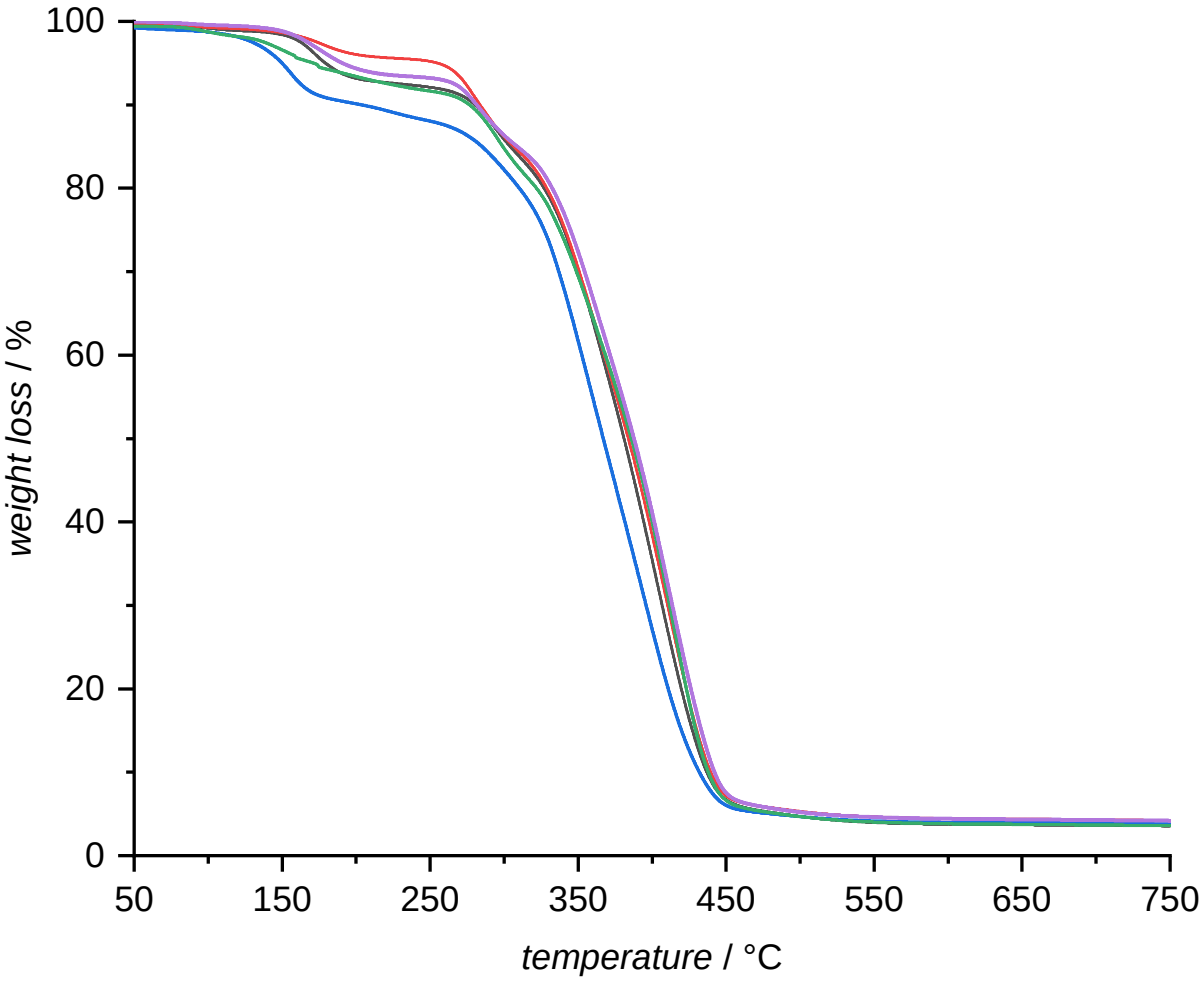

Fig. S34: TGA of typical copolymers consisting of 20% **PEMA** and various amounts of BMA and MMA, clearly showing decomposition after 140 °C.

S10 Nanoindentation

Table S5: Table listing the data shown in Fig. 3 (main document).

BMA [%]	MMA [%]	PEMA [%]	T_{cure} [°C]	t_{cure} [min]	E_r [GPa]	*Hardness* [MPa]
30	55	15	45	0	2.97 ± 0.49	34.3 ± 3.9
30	55	15	45	1	4.58 ± 0.02	165.3 ± 1.8
30	55	15	45	2	5.14 ± 0.02	263.8 ± 3.6
30	55	15	45	5	5.27 ± 0.03	294.3 ± 5.7
30	55	15	45	10	4.94 ± 0.3	286.1 ± 2.1

S11 Rheology

The tested photoresist in Fig. 2 consists of 50% MMA, 33% BMA and 17% PEMA, with a number average molecular weight of 13800 g mol^{-1} ($Đ$ = 1.92). For the experiment in the presence of a small additional crosslinker moiety, the same polymer sample was dissolved in dichloromethane and diethyl tetraethyleneglycol difumarate (1.00 eq) was added. The experiment was carried out after solvent evaporation and successive drying of the remaining sample.

S12 Light Sources

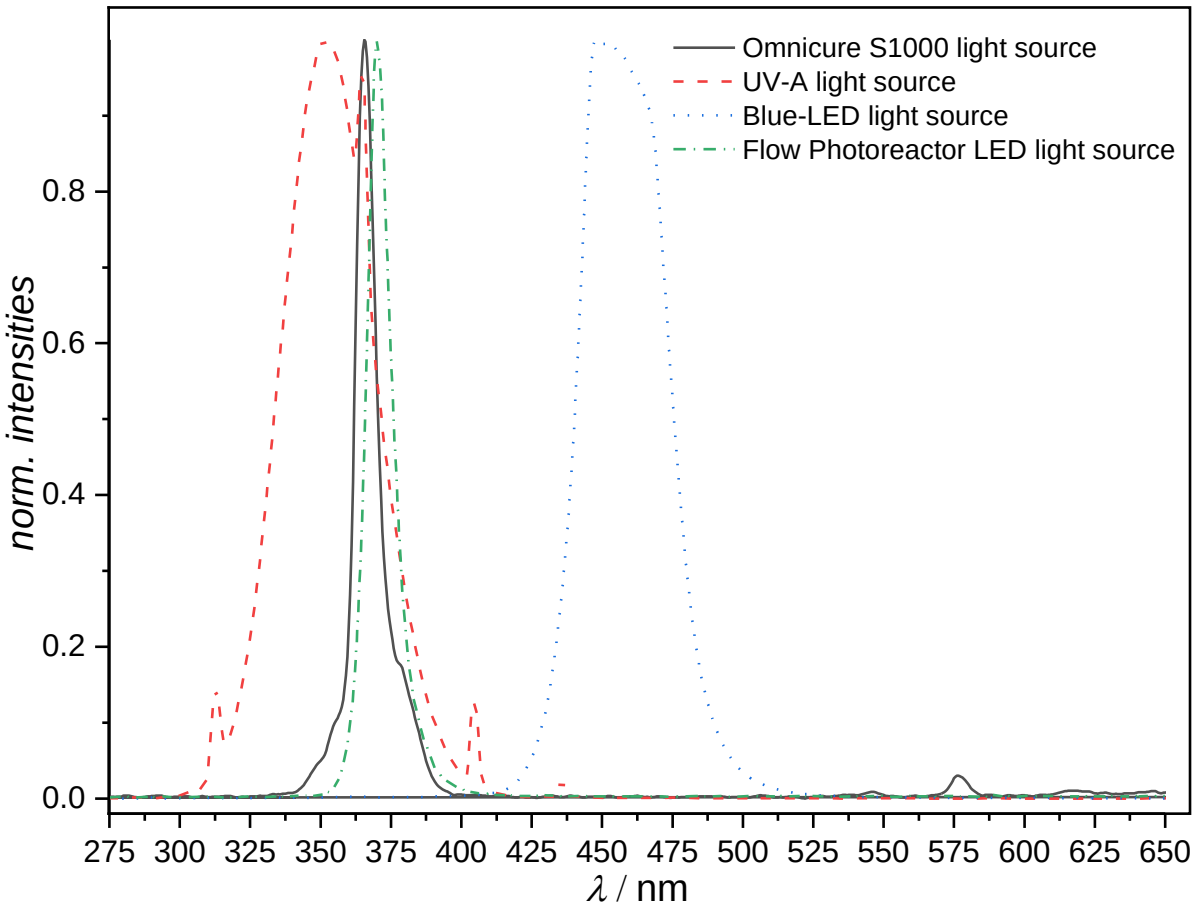

Fig. S35: Omnicure S1000 Emission Spectrum, equipped with a 365 nm bandpass filter (black); UV-A light source emission spectrum utilized for curing (red), blue-LED emission spectrum utilized for photopolymerization (blue) and flow photoreactor 365 nm LED emission (green).

S12 Photoreactor

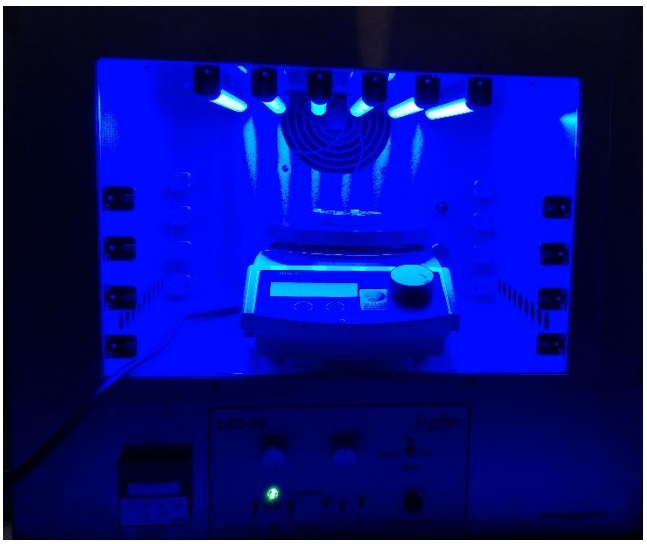

Fig. S36: Image of the photoreactor that was utilized for photpolymerization and curing experiments is exemplary shown, equipped with 6 Blue LEDs for top irradiation.

S13 References

[1] K. K. Oehlenschlaeger, J. O. Mueller, N. B. Heine, M. Glassner, N. K. Guimard, G. Delaittre, F. G. Schmidt and C. Barner-Kowollik, *Angew. Chem. Int. Ed.,* **2013**, *52*, 762.

[2] T. Pauloehrl, G. Delaittre, V. Winkler, A. Welle, M. Bruns, H. G. Börner, A. M. Greiner, M. Bastmeyer and C. Barner-Kowollik*, Angew. Chem. Int. Ed.*, **2012**, *51*, 1071.

[3] T. K. Claus, B. Richter, V. Hahn, A. Welle, S. Kayser, M. Wegener, M. Bastmeyer, G. Delaittre, C. Barner-Kowollik *Angew. Chem.,* **2016**, *55,* 3817.